Charles University

Faculty of Science

Department of Physical and Macromolecular Chemistry

Institute of Macromolecular Chemistry AS CR, v.v.i.

Department of Nanostructured Polymers and Composites

„MULTICOMPONENTAL POLYURETHANE SYSTEMS WITH TARGETED PROPERTIES. PREPARATION AND CHARACTERIZATION“

Dissertation work

Eng. Magdalena Serkis-Rodzeń, MSc

Supervisor: Eng. Milena Špírková, CSc

Prague 2017

Univerzita Karlova

Přírodovědecká fakulta

Katedra fyzikální a makromolekulární chemie

Ústav makromolekulární chemie AV ČR, v.v.i.

Oddělení nanostrukturovanych polymeru a kompozitu

„VÍCESLOŽKOVÉ POLYURETHANOVÉ SYSTÉMY S CÍLENÝMI VLASTNOSTMI. PŘÍPRAVA A CHARAKTERIZACE“

Disertační práce

Mgr. Ing. Magdalena Serkis-Rodzeń

Školitel: Ing. Milena Špírková, CSc

Praha 2017

Prohlášení:

Prohlašuji, že jsem závěrečnou práci zpracovala samostatně a že jsem uvedla všechny použité informační zdroje a literaturu. Tato práce ani její podstatná část nebyla předložena k získání jiného nebo stejného akademického titulu.

V Praze, 27.03.2017

Declaration:

Hereby I declare that I have worked out this doctoral thesis independently, and I have fully cited all sources used. This work has not been used in order to gain any other academic degree.

Prague, 27.03.2017

Magdalena Serkis-Rodzeń

Acknowledgements

First of all, I would like to express my gratitude to my supervisor for the opportunity to work on this interesting research topic. I am thankful for her time and sharing her knowledge and experience not only about polymer science, but also about AFM method.

I would like to express my thankfulness to all my colleagues, who helped me in my research.

My special thanks go to my family. I thank my favorite person in the world, my husband, for believing in my abilities, inspiring me and understanding.

Thanks to my younger brother for being always on my side.

I would like to thank my dear parents for their unconditional love and constant support. *Dziekuję moim drogim rodzicom za bezwarunkową miłość i niekończące się wsparcie.*

Abstract

Thermoplastic polyurethanes (PU) have been widely used for many applications due to their excellent functional properties, recycling included. PUs prepared in this Thesis are based on polycarbonate macrodiols and other linear components, leading to linear solely aliphatic materials.

The main part of this study is focused on synthesis and analysis of polyurethane water dispersions (PUDs) and PUD-based films. The novelty of presented herein research involves ecofriendly method for preparation of thermoplastic PUs based on polycarbonates. The PU nanoparticles dispersed in water were measured by scattering methods, whereas the final films were characterized for their morphology and mechanical, thermal and water resistance. A balance between hydrophilic and hydrophobic parts of PUs for the particles stability and the films properties was investigated as well.

The PUDs were blended with two types of colloidal silica for improve of the PUD-based films resistances with simultaneous preserving of their thermoplastic character. More significant enhancement was observed for the organic-inorganic nanocomposites containing silica with smaller particles, due to creation of higher physical crosslinking density between the nanofiller and PU matrix.

We modified the acetone process of PUDs preparation by elimination of the chain extension step and using of water both as a medium and a crosslinker, leading to more ecological, simpler and cheaper method. We proposed the mechanism of linear and water-crosslinked PU nanoparticles self-assemblies in acetone and in water in two steps of the synthesis.

The second part of this Thesis consists of hydrolytic degradation study of PU elastomers under conditions mimicking the physiological environment. Biostable and biodegradable PUs with or without the degradable unit in PU backbone were investigated for their microstructure by atomic force microscopy and scanning electron microscopy.

Key words: polyurethane water dispersion, thermoplastic polyurethane, polycarbonate macrodiol, organic-inorganic nanocomposite, self-assembly

Contents

List of abbreviations

AFM	atomic force microscopy
BD	butane-1,4-diol
DLL	D,L-lactide-based oligomeric diol
DLS	dynamic light scattering
DMPA	2,2-bis(hydroxymethyl) propionic acid
DMTA	dynamic mechanical thermal analysis
DSC	differential scanning calorimetry
FTIR	Fourier transform infrared spectroscopy
HDI	1,6-diisocyanatohexane
HS	hard segment
PBS	phosphate-buffered saline
PCD	polycarbonate macrodiol
PU	polyurethane
PUD	polyurethane water dispersion
SEM	scanning electron microscopy
SLS	static light scattering
SS	soft segment
TEA	N,N-diethylethanamine
TG	thermogravimetric analysis
VOC	volatile organic compound

List of symbols

T_g	glass transition temperature
T_m	melting temperature
R_H	hydrodynamic radius
D	diffusion coefficient
k_B	Boltzmann constant
η	solution viscosity
μ_E	electrophoretic mobility
ζ	zeta potential
ε	dielectric constant
R_θ	Rayleigh ratio
i_θ	scattered light intensity
I_0	incident beam intensity
M_w	weight-average molecular weight
R_g	radius of gyration
A_2	second virial coefficient
δ	phase angle
E', G'	storage modulus
E'', G''	loss modulus
E	Young's modulus
σ_b	tensile strength
ε_b	elongation at break

1. Introduction

1.1. History of polyurethanes

In 1937 German professor Otto Bayer and coworkers at I. G. Ferbenindustri first discovered fiber-forming polyurethane as a result of searching for a proxy for Nylon discovered in 1935 and covered by patent held by E. I. DuPont. The initial materials were synthesized via reaction of aliphatic diisocyanates with diamines. The obtained polyureas were infusible and hydrophilic.[1-3]

The first patent on polyurethane was awarded in 1938 by Rinke and Associates, who successfully reacted 1,8-diisocyanatooctane with butane-1,4-diol to form esters of carbamid acid, called polyurethanes.[4]

The industrial scale production started in 1940, when DuPont and ICI recognized the desirable elastomeric properties of PUs. In this process water was a chain extender and used diisocyanate was 1,5-diisocyanatonaphtalene. Intensive development of PUs was impacted by World War II due to the lack of natural rubber in this time. In 1950's and 1960's progress in modifications of PUs was achieved as a production of Vulkallan rubbers, Spandex fiber called Lycra, Estane and so on. Nowadays, PUs are used in broad range of applications because of their excellent mechanical properties and biocompatibility.[2-5]

1.2. General information

Polyurethanes belong to the most important class of polymer materials. Term *polyurethane* refers to polymers containing a plurality of urethane group (-NHCO-O-) on the macromolecular chain. Thus, under this name, beside urethane linkages, other functional groups may be incorporated into the polymer structure. As a consequence, PUs with target properties, varying from rigid hard thermosets to soft elastomers, may be prepared.[3,4,6]

Polyurethanes are used in wide area of commercial applications. In 2007, the world production of PUs had a volume nearly 12 million tons annually, classifying them as one of the main polymeric materials.[7,8]

The major benefits of PUs are: high impact strength at low temperatures, ability of foams production, controllable hardness and resistance to oxidation, abrasion, ozone, humidity and tear propagation. However, the flammability and low stability at temperatures above 90 °C are factors reducing PU applicability. The main fields of applications for PUs are automotive industry, bedding, insulations, furniture, textiles, medicine, coatings and adhesives. Rigid PU foams are used for insulation in home refrigerators and construction industry, whereas flexible foams found applications as mattresses, packaging materials and in furniture production. Other PU materials may be classified as cast able resins and thermoplastic elastomers used mostly for the footwear, sport equipment and electrical industry. Since PUs combine excellent mechanical properties with good blood compatibility, they found applications as biomaterials as well. They are used for example as drug delivery systems, biostable implants and biodegradable materials supporting growing of new tissue.[3-5,8-10]

1.3. Synthesis and structure of polyurethanes

1.3.1. Chemistry of polyurethanes

Polyurethanes are synthesized in step growth polymerization by the reaction between organic isocyanate (-N=C=O) and active hydrogen compounds (R-OH) or (R-NH_2). In this reaction, bifunctional monomers react stepwise to produce long chains of monomer residues. Since no small molecule, such as CO_2 or water, is eliminated during the reaction, it can be classified as polyaddition.[4-6]

The methods for preparation of PUs can be consider according to the reaction medium (bulk, organic solvent, water) and the addition order of components (one-step or prepolymer method). In the *one-step,* also called *one-shot polyaddition procedure,* all reagents (diisocyanate, macrodiol and chain extender) are reacted at once (see Scheme 1a)). This procedure is commonly used in industry due to short time of reaction, ease to perform and high reproducibility. However, this method does not provide control required to obtain regular block sequences. In the one-shot technique the difference in reactivity of isocyanate groups and different OH groups of a macrodiol and a chain extender may produce a mixture of oligomers diisocyanate-chain extender and diisocyanate-macrodiol.[3,5,6,11]

In contrast, in the *two-step polymerization technique* at first a macrodiol reacts with an excess of a diisocyanate to form an isocyanate-terminated low-molecular weight prepolymer. The second step constitutes chain extension with a short diol or diamine (see Scheme 1b)), which produces a multiblock copolymer of the $(AB)_n$ type with the increased overall molecular weight. Because this method is more controlled and produces fewer side reactions than the *one-step procedure*, is commonly used for synthetize of biopolyurethanes.[3,6]

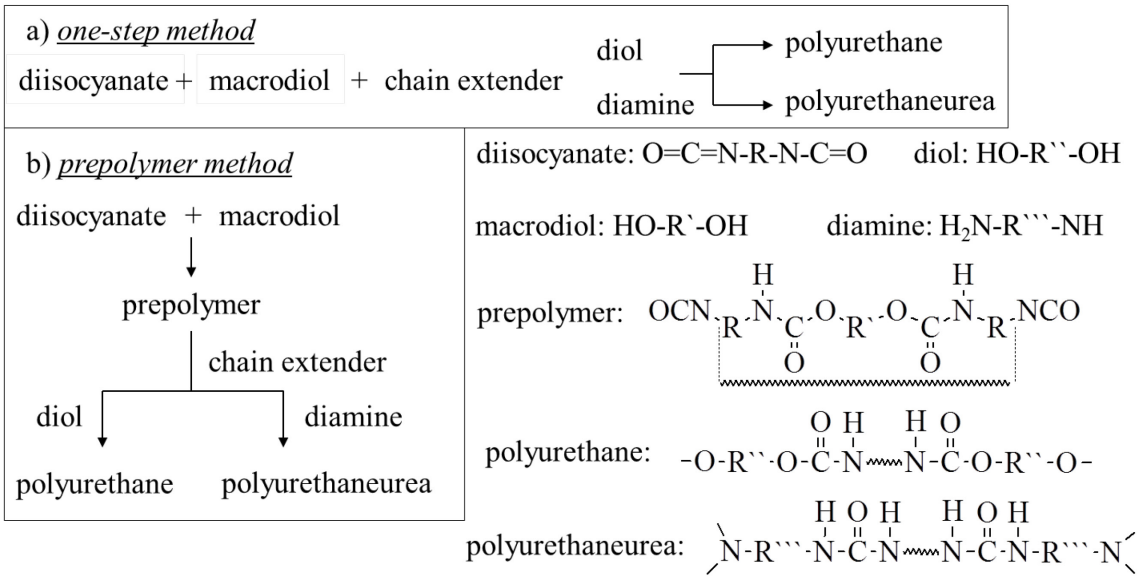

Scheme 1. Preparation of PUs based on: a) one-step method, b) prepolymer method.[3,5,6]

1.3.2. Segmented structure of polyurethanes

Since PU elastomers are formed by the reaction of a diisocyanate with a long-chain diol and a small molecule chain extender, they may be considered as segmental copolymers. The soft segment (SS) is usually formed from polyether, polyalkyldiol or polyester of molecular weight between 400 and 5000 g·mol^{-1} with low T_g. The SSs constitute amorphous domains, which impart rubber-like behavior and elastomeric properties of PUs. On the other hand, hard segments (HSs) are the reaction products of a diisocyanate with a chain extender. The HSs are either glassy or crystalline domains with a high T_g or a high T_m and act as filler particles, reinforcing the SS matrix.[2-4,6,12-14]

Although there is some degree of mixing between SSs and HSs, the segments segregate to form a pseudo-two-phase structure. This behavior is a result of intrinsic incompatibility and thermodynamic immiscibility between the segments caused by their

different polarities and free energy. The HSs tend to cluster or aggregate and provide physical crosslink sites for the soft microphase. The extent of SS/HS phase separation plays an important role in determination of PU solid-state properties, such as vapor permeability, hydrolytic resistance, thermal stability and mechanical properties. The degree of microphase segregation may be regulated by selecting of SS and HS with proper lengths and sequence of length distribution, molecular weight, chemistry and possibility to form hydrogen bonding. Thermal history of PUs and the method of preparation are also known to affect the degree of phase separation/mixing and organization of hard domains. For example, PUs containing 15-40 wt% of HS are typically soft and rubbery elastomeric materials, whereas PUs with 40-60 wt% of HS are tough elastomers. The degree of microphase separation can be analyzed by atomic force microscopy, electron microscopy, small angle X-ray scattering and small angle neutron scattering.[2,5,7,13,15]

1.3.3. Raw components used in the synthesis

1.3.3.1. Isocyanates

An isocyanate is the first essential component of PU. Molecules containing two isocyanate groups are called diisocyanates, whereas compounds with more than two -NCO groups belong to polyisocyanates.

Two main classes of isocyanates used in synthesis of PUs are aromatic and (cyclo)aliphatic types. Aromatic isocyanates in comparison to aliphatic isocyanates are more reactive and lead to stiffer PU chains with a higher T_m, but their oxidative, hydrolytic and ultraviolet resistances are lower. They are mostly used in biomedical PUs. The most common aromatic isocyanates are 2,4-diisocyanato-1-methylbenzene (TDI) (consisting of an isomeric mixture of the 2,4-TDI and 2,6-TDI) and 1,1'-methylenebis(4-isocyanatobenzene) (MDI). Although MDI is more expensive than TDI, it has higher reactivity and may lead to polymers with better physical properties. Aliphatic and cycloaliphatic isocyanates find wide use in coating applications due to their higher light stability. Typical examples of this class are 1,6-diisocyanatohexane (HDI), 5-isocyanato-1-(isocyanatomethyl)-1,3,3-trimethyl-cyclohexane (IPDI) and 1,6-diisocyanato-2,2,4-trimethylhexane (TMDI).[2,3,5,6]

Isocyanate group is highly reactive toward nucleophilic reagents due to the electro-positive character of the carbon atom. This electro-positivity is higher in aromatic than in aliphatic diisocyanates, because the benzene ring drains the electron cloud of the nitrogen atom, making the carbonyl carbon more exposed to the nucleophilic attack. Electron-donating substituents present near the C atom in the –NCO group can slow down the rate of isocyanate reactions. The reduction of the reaction rate may be also caused by branched groups and bulky side groups in aliphatic isocyanates or by bulky groups in the orto position in the case of aromatic isocyanates, due to formation of steric hindrance. The reactivity of the second –NCO group in diisocyanates is decreased after the reaction of the first one. These differences in the reaction rates are reduced when the –NCO groups are separated by aromatic rings or aliphatic chain.[3,4,15,16]

Scheme 2 summarizes the reactions of –NCO group with different components. The main way of PU synthesis is the reaction of the isocyanate group with –OH terminated molecule (Scheme 2a)). In this case the rate of reaction of primary alcohols is around three times faster in comparison to secondary alcohols and around 200 times faster than in the reaction of tertiary alcohols. If –NCO groups are present in excess, they can take a part in a reversible reaction with urethane groups to form allophanate (Scheme 2b)). The allophanate linkages are junction points and, as a result of crosslinking, can improve mechanical properties of obtained materials. However, they can dissociate to urethane and isocyanate, depending on temperature and the type of used compounds.[3,15,17-20]

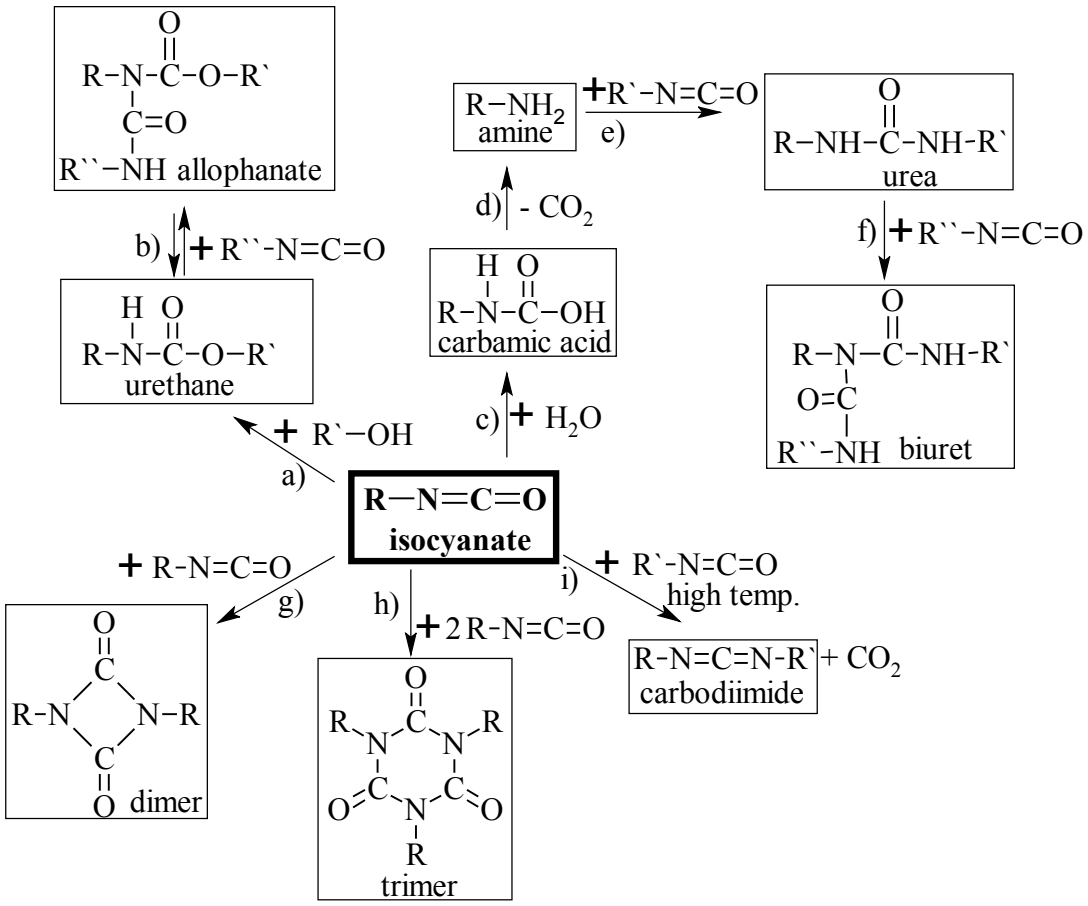

Scheme 2. Reactions of isocyanate group.[3,15,19]

Isocyanates can also react with water (Scheme 2c)). At the first step unstable carbamic acid is formed (Scheme 2d)), which decompose to amine (Scheme 2e)). Beside the amine product, also carbon dioxide is liberated. This process is widely used in a production of PU foams, where CO_2 acts as a blowing agent. Amines react with isocyanate to form bifunctional urea linkages (Scheme 2f)), which means that this is a chain extension process. Urea groups further can react with the –NCO groups and yield trifunctional biuret, which increases a crosslinking density. Biuret linkages are more stable than allophanate, but still thermally labile. Isocyanate groups can also react with each other to dimer (uretidione) or trimer (isocyanurate) formation (Scheme 2g) and h), respectively). Cyclotrimerization is used to produce PU coatings and rigid, high temperature resistant foams. Other possible reaction of the –NCO group with another –NCO group is carbodiimide formation (Scheme 2i)). Carbodiimide groups are thermally and hydrolytically stable.[3,15,19-22]

1.3.3.2. Polyols

Di-hydroxy terminated polyols are called macrodiols. These compounds form soft segments, responsible for elastomeric properties of PUs. The type and length of macrodiol play an important role in the mechanical and physico-chemical properties of PU materials. Generally, long high-molecular weight polyols lead to PU elastomers, whereas short low-molecular weight macrodiols produce rigid plastics. The most important polyols are polyester (polycarbonate, polycaprolactone), polyether and polybutadiene polyols.[2,4,9]

Polyether polyols are mostly used as solvent-free coatings, but their applications are limited to interior use or production of primers, due to high oxidative degradation of polyether chains. However, they provide good mechanical and hydrolytic stability of formed PUs. Polyester polyols are synthesized in the polycondensation reaction between polycarboxylic acids with an excess of polyols. PUs based on non-aromatic polyesters yield good weather and UV stability, whereas aromatic polyester diols tend to yellowing when they are exposed to light. Due to their properties, aliphatic polyester polyols found applications in a wide area of PU coatings, used for cars, aircraft, industrial machinery and so on.[3,9]

Polycarbonate polyols

Polycarbonate polyols belong to a special class of polyesters, having much higher oxidative resistance than polyether-based PUs. Over other polyesters, they are more UV and hydrolytic stable, due to formation of unstable derivative of carbonic acid in the reaction of polycarbonate groups with water. This derivative decompose to nonacidic species, which prevent the acid catalyzed decomposition of PUs.[23,25]

There are several methods for preparation of polycarbonate polyols, including the reaction of diols with phosgene, dioxolanones, bischlorocarbonic acid esters, diaryl-/dialkyl-carbonate or urea. The simplest is the reaction between phosgene/carbonate monomer with a diol (Scheme 3a)). However, this method is not recommended due to using of phosgene, unfriendly for the environment. The best technique for preparation of high-molecular weight polycarbonate diols is the condensation of dimethyl carbonate and diols (Scheme 3b)). This procedure needs the optimum reaction temperature, at which methanol - dimethyl carbonate azeotrope formation is minimalized. The copolymerization

of epoxides and carbon dioxide (Scheme 3c)) gives alternative polycarbonates – the polyalkylene carbonates. The main problem in this process is the cyclic carbonate production. The undesired product formation is minimalized by using of proper catalysts, for example cobalt - selen complexes or dimagnesium catalysts.[4,25-27]

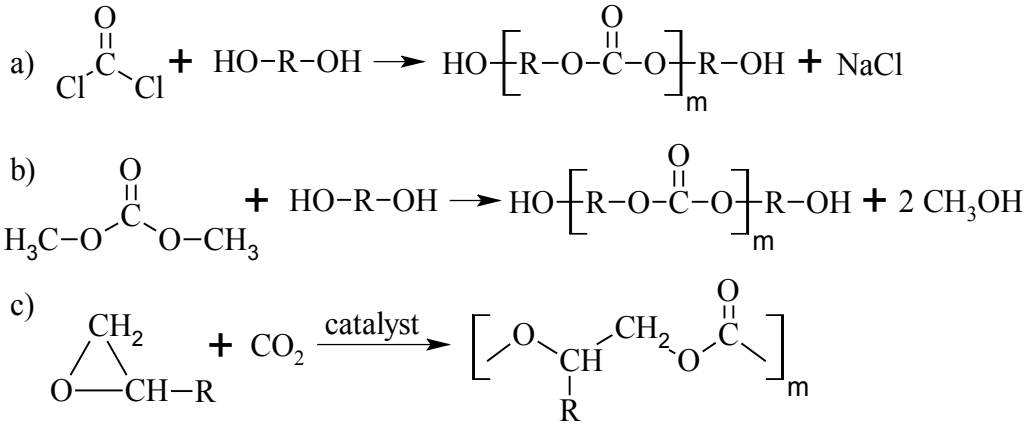

Scheme 3. Preparation of polycarbonate diols using: a) phoshene, b) dimethyl carbonate, c) alkoxylate.[25-27]

In spite of relatively high costs of polycarbonate diols, they found a wide area in PU applications due to their good mechanical properties and better resistance to organic solvent, hydrolysis and oxidative degradation compared to polyethers. In recent years, biostable and mnbiocompatible aromatic polycarbonate macrodiols containing bisphenol A, have been used in medical applications, such as implants, blood pumps, heart valves and so on. However, their low solubility limits their coating applications. Therefore, aliphatic polycarbonates are mostly used as PU adhesives, coatings and dispersions for medical, packaging and shoe industries.[9,23,25,28-32]

1.3.3.3. Chain extenders

Chain extenders are low-molecular weight (from 40 to 300 g·mol^{-1}) bifunctional compounds containing active hydrogen. Their main function is an extension of HS. The addition of chain extenders results in increasing of molecular weight and hydrogen bonding density. Thus, as a result of local phase ordering, the possibility of crystallinity increases. Moreover, segregation of HSs causes increasing of modulus and T_g, which gives possibility in prediction of PU softening point and temperature limits for working. The lack of a chain extender in the PU structure leads to physically poor materials, often without microphase separation.[6,33-36]

Chain extenders can be classified into two categories: aliphatic diols and diamines and the corresponding aromatic diols and diamines. Diamine chain extenders are highly reactive and lead to formation of urea links, resulting in PU crosslinked with biuret groups. These chain extenders produce stiffer HSs and the obtained PUs have higher hardness, modulus and tensile strength in comparison to PUs based on diols. Aliphatic diamines are more often used than aromatic diamines due to their lower reactivity and less production problems. However, it was found that diamines with a substituent in the orto position in the benzene ring provide optimum reactivity and good physical properties of final PUs.[3,6,37,38]

A diol chain extender leads to softer PUs than while using diamines. Generally, aromatic diols lead to tougher elastomers compared to aliphatic diols, due to their less flexible units. Thermoplastic PUs can be obtained only when linear diol is used as a chain extender. Branching diols lead to formation of crosslinks, so the resulted PUs cannot be re-processed by thermal treatment. The most common diol chain extender is butane-1,4-diol (BD), extensively used for medical applications. Moreover, mixture of chain extenders is also possible to use.[3,38,39]

1.4. Thermoplastic polyurethanes

Thermoplastic polyurethane elastomers (TPUs) are linear, block copolymers combining semi-crystalline or glassy thermoplastic character and soft rubber elasticity. At room temperature, TPUs possess crosslinked rubber behavior, due to incompatibility of HS and SS, leading to the microphase separation. However, at temperature above T_g of the HS, the polymer viscous melt is formed, which enables the melt-processing of TPUs. This behavior is illustrated in Fig. 1. The re-cooling of the melt results in subsequent segregation of HSs into SSs. Segmented TPUs contain 60-85 wt% of SS.[40-44]

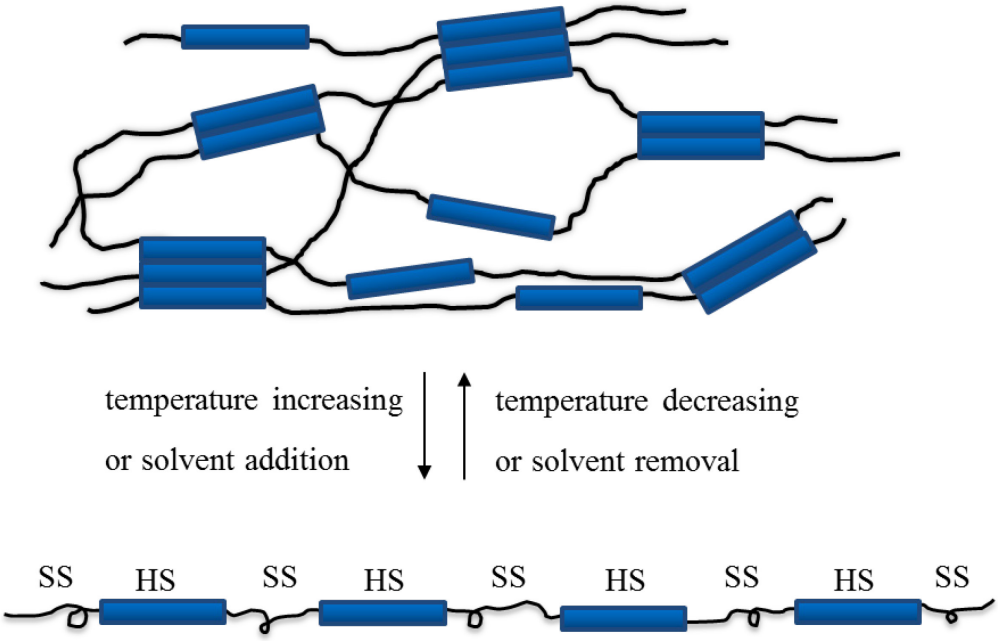

Figure 1. TPU chain behavior under processing.[46]

To obtain thermoplastic PUs without or with only low branching, the functionalities of used raw components should be around 2 in total. Thus, an NCO:OH molar ratio, called the isocyanate index, about 1 is usually used in the synthesis of TPUs. To prepare partially crosslinked TPUs, a small excess of NCO (0.1-0.2 %) is used, whereas post-curable polymers have NCO:OH ratio between 0.98 and 0.99. Theoretically, if the isocyanate index is equal to one, the chemical crosslinking is negligible and the rubber-like behavior depends mostly on physical networks, which is called "virtual crosslinking". In practice, an NCO:OH ratio between 1.02 and 1.05 is used for preparation of TPUs, due to side reactions of an isocyanate with water contained in components and in the air. The substantial excess of NCO leads to formation of chemical networks through allophanate and biuret groups. However, chemical crosslinks have a significant influence on PU thermal stability, which can be sorted as follows: isocyanurate > urea > urethane > biuret > allophanate. Thus, increasing of chemical crosslinking density limits a thermal re-processing of PUs. The elastomeric properties of PUs depend on both physical and chemical networks. Increasing of chemical crosslinking causes changes in PU morphology and their hardness. This can be explained by increasing of attraction forces between HSs, leading to increasing of tensile strength and decreasing of elongation at break.[22,29,38,44-48]

Although TPUs are materials with high elongation and flexibility, they have some limitations due to sensitivity to water, UV radiation, alcohols, nitrogen oxide, microorganisms and strong alkalis. They are mostly used for the production of adhesives, coatings, engineering materials and films, by extrusion and injection techniques. TPUs found applications as alternatives to solvent-borne PU adhesives due to good strength after their fast crystallization. Unfortunately, above T_m of the crystalline phase, they lose their strength. However, addition of short diol chain extenders improves thermal stability of TPUs. Thermoplastic PUs are versatile materials used in the following areas: a) energy, as cable jackets; b) automotive painting; c) electronics for mobiles and computers; d) petrochemical; e) textile; f) footwear; g) sport equipment; h) medical devices and scaffolds for tissue engineering; i) furniture; j) aerospace; k) other industrial products.[36,42,46,49-55]

1.5. Polyurethane water dispersions

1.5.1. History of waterborne polyurethanes

Polyurethane water dispersion (PUD), also called waterborne polyurethane, is a colloid system, where PU nanoparticles are dispersed in an aqueous medium. After development of PUs, researchers sought to obtain water soluble polyurethanes with a high amount of hydrophilic groups. In the first approach, strongly basic PUs were prepared. However, they were not possible to use in commercial applications because of too high hydrophilicity. Later reaction of prepolymers with a diamine water solution in the presence of surface active agents led to unstable dispersions. Moreover, relatively large particle size distribution caused problems in film formation and deteriorated water resistance.[56-58]

PUDs containing hydrophilic ionic groups in the PU backbone, have been available since the late 1960s, and since the early 1970s they have been commercial products. Because environmental concerns tend to production of non-solvent materials and reduction of VOCs (volatile organic compounds), PUD market is still growing. The advantages of new water-borne PUDs are their performance similar to some solvent-borne systems and possibility of processing with similar equipment. The growing interest in PUDs resulted in over 1000 patents since the past 20 yers.[56-60]

1.5.2. Types of PUDs

Conventional polyurethanes are hydrophobic and immiscible in water. Thus, incorporation of salt forming or hydrophilic groups into the PU backbone is necessary to make them self-dispersible. PUDs can be classified according to their charge, as ionomers (Fig. 2), containing ionic groups anchored in PU backbone via covalent bonds, or non-ionic PUDs. In the case of ionomer, the ionic groups act as internal emulsifier. Frequently used pendant groups in PUDs include acid functional forms, tertiary amine-based cationic groups or non-ionic sulfactants.[9,56,59]

1.5.2.1. PU cationomers

Cationic PU ionomers (Fig. 2a)) are prepared in the reaction of NCO-terminated prepolymer and low-molecular weight tertiary amine containing hydroxyl groups. They can incorporate various cations into their structure, for example sulfonium, ammonium or phosphonium, together with proper counter-ions. The suitable ionic pair is formed by neutralization of amine with acid or in the reaction with benzyl chloride, alkyl chloride, dimethyl sulfate or another polymer containing chlorine groups.[8,56,61]

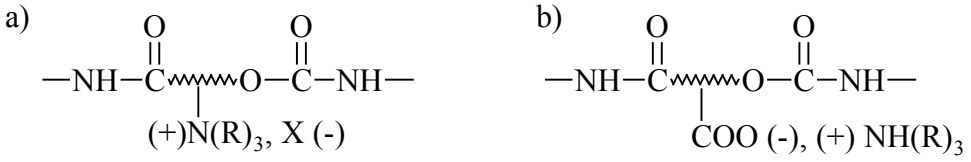

Figure 2. Ionomeric types of PUDs: a) PU cationomer, b) PU anionomer.[8,56]

The increasing number of ionic groups in cationic PUs causes increasing of their hydrophilicity, flexibility, mechanical strength, permeability and selectivity of PU membranes. They show good adhesion to anionic substrates and porous surfaces. Due to this fact, PU cationomers found applications as coatings for glass, PVC and rubber. They are important retaining agents for natural leather, because of color improvement after the dyeing. Cationic PUs are also used as additives during the coagulation process, binders between flexible and rigid surfaces and in a production of poromerics.[8,56,61-63]

1.5.2.2. PU anionomers

Anionic PU ionomers (Fig. 2b)) are predominant in commercial preparation of PUDs. Acidic functional groups, the most often HSO_3^- or COO^-, are incorporated in their chains. It was found that polycarboxylates give good hydrophobicity, whereas polysulfonates provide PUDs with excellent stability.[8,56]

There are three steps of PU anionomers preparation. At first, as a result of reaction between a diol and an excess of diisocyanate, prepolymer is formed. In addition, dihydroxyl carboxylic acid is reacted into the prepolymer. The most often used ionic center is DMPA (2,2-bis-(hydroxymethyl)propionic acid) due to steric hindrance of the carboxyl group, preventing its reaction with –NCO. In the second stage, COOH groups are neutralized with a basic material to obtain anionic hydrophilic centers. As neutralizing agent are used N,N-dimethylmethanamine (trimethylamine), N,N-diethylethanamine (triethylamine), ammonia, NaOH, KOH, or LiOH. The last step of the PU anionomer preparation covers chain extension of the prepolymer. As a result, the residual –NCO groups are transformed into urea and a stable PUD is obtained after water addition. Further evaporation of water leads to formation of the PU film.[5,8,9,56,57,64]

PU anionomers are used for electronic and optic applications as dopant ion and macromolecular electrolyte, due to their considerable conductivity and polarity. They are also biomaterials for preparation of anticoagulants for delay clotting times or substances with antimicrobial properties. Moreover, anionic PUs can be employed as temporary binders for ceramic materials.[8,64-68]

1.5.2.3. Non-ionic polyurethanes

PU non-ionomers have non-ionic hydrophilic centers built into the polymer backbone, without any ion dangling on PU chain. In this type, a part of hydrophobic polyols is replaced by hydrophilic polyethylene oxide. The hydrophilic segments terminate PU chain or are attached as lateral groups. Unlike the ionic PUs, stabilized by formation of electrical double layer, the non-ionic PUs are stable via entropic repulsion mechanism between the PU chains.[56,57,69-72]

The main disadvantage of nonionomers is necessity of incorporation of high number of hydrophilic parts to obtain stable PUDs, which leads to water sensitive films, swellable or even soluble in water. Moreover, this type of PUD causes problems in the

emulsification process, due to possibility of thermocoagulation and low heat resistance, caused by decreasing of hydrophilic segments solubility in water at higher temperatures.[56,70]

Nonionic PUDs, compared to ionic types, are more alkali, acid, electrolytes, strong shear forces and freezing resistant. These features provide their applications in a production of synthetic leather surfactants, pigments, thickener, fillers and other. On the other hand, ionomers have higher strength, modulus and hardness than the non-ionic types. Fortunately, combination of non-ionic hydrophilic segments and ionic groups leads to synergistic effects on the PUD stability, fine particle size and reduction of the overall hydrophilic part content.[56,69-71,73]

1.5.3. Dispersion and film formation

1.5.3.1. Formation of PU nanoparticles dispersed in water

The dispersity/mixing stage in water is an important factor affecting PUD stability and their final properties. It was found that neutralization with amine of fully reacted PU in an organic solvent (see Scheme 4a)) causes increasing of the mixture viscosity due to creation of micro-ionic lattices. These forms are results of intra- and inter- molecular electrostatic interactions between positive and negative ions in ionomeric PUDs. Thus, repulsion and elastic forces along PU chain lead to pseudo-crosslinking formation, which is responsible for increasing of the mixture viscosity.[74-76]

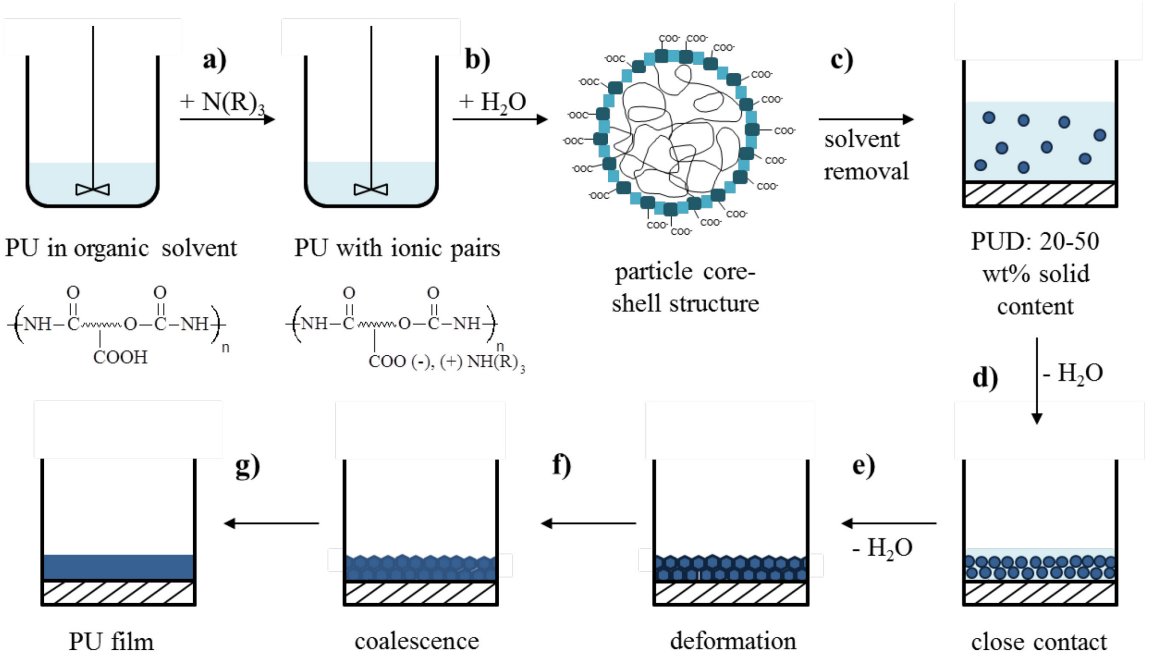

Scheme 4. Formation of anionic PUDs and PUD-based films: a) neutralization of carboxylic groups and formation of ionic pairs, b) water addition: re-arrangement of HSs and SSs leading to formation of core-shell structure, c) organic solvent removal giving waterborne PU, d) water evaporation leading to increasing of PU concentration, e) further water removal: deformation of soft particles, f) coalescence and inter-diffusion, g) continuous PU film.

The contraction of van der Waals attractions between dispersed PU nanoparticles in water takes place by different stabilization mechanisms for ionomeric and non-ionomeric PUDs. In the case of PU ionomers an electrical double layer between the ionic groups bounded to PU backbone and their counterions migrating to the water phase is formed. As a result, the particles repeal from each other, forming a stable PUD.[9,56]

In contrast, non-ionic PUs are stabilized in water by an entropy effect, as mentioned above. In these PUDs hydrophilic segments built into the polymer chains, stretch and penetrate the aqueous phase. However, the conformational freedom of polyethylene oxide chains is limited by approaching of the particles. This behavior is thermodynamically unfavorable and causes repelling of the nanoparticles, when they approach too close to each other. Therefore, the repulsion is a spontaneous movement caused by a reduction of entropy.[9,56]

There are several steps of transformation of an organic PU solution into a PUD. The initial water addition causes sharp increasing of viscosity due to reduction of ionic groups. As more water is added, the viscosity increases to maximum, although the solids amount decreases. This can be explained by reduction of solvation sheath of the hydrophobic segments due to decreasing concentration of organic solvent. Subsequent water addition leads to turbidity, producing initially dispersed phase. As a result of further increasing of turbidity, the viscosity decreases. This behavior is caused by re-arrangement of PU segments and creation of core-shell structure, where hydrophobic PU parts are surrounded by hydrophilic groups (see Scheme 4b)). The re-arrangement leads to formation of microspherical PU particles dispersed in the water phase. The last step for obtaining of a waterborne PUD is organic solvent removal.[56,75,77]

The structure of PU nanoparticles dispersed in water is similar to polymer molecular coils in colloidal aqueous solutions. In contrast to emulsifier-stabilized dispersions, in ionic PUDs the particle phase borders are not sharply defined. This fact causes problems with determination of their size. The size of PU particles in water depends on the PU molecular weight, hydrophilicity, the mobility of PU chains, the ionic groups content, the ratio of water to organic solvent, temperature and mixing conditions, the degree of neutralization and type of neutralization agent. It was found that the particle size decreases with increasing of PU hydrophilicity, ionic centers amount, degree of neutralization and force of mixing. Moreover, the metal cations favor PUDs with smaller particles than ammonium cations. Further, lower reaction temperature leads to decreasing of the particle size due to disruption of hydrogen bonding formation, resulting in separation of the PU chains into smaller polymer fragments.[9,56,74,75,78]

The particle size of PUDs is varied from 10 to 500 nm and significantly influences the dispersion stability. The nanoparticles larger than 100 nm are generally unstable in water due to sedimentation. Therefore, PUDs with smaller particles are widely used because of their better stability and high surface energy, leading to stronger driving force for PU film formation. The particle size affects also the appearance of PUDs, from opaque sol with small nanoparticles to a milky white dispersion containing large particles. Common PUDs have a pH from 6 to 9, solids content between 35 and 50 % and viscosity around 100 mPa·s.[9,56,79]

1.5.3.2. Film formation

PUDs feature excellent polymer film-forming properties, influenced by temperature. It was found that there is no phase separation on organic and water phase between upper critical solution temperature depending on PU hydrophilicity and lower critical solution temperature defined by hydrophobic nature of PUs. There are several possible methods for improvement of the film-forming properties, such as addition of coalescent solvents with high boiling temperature or plasticizers or increasing of drying temperature.[56,80]

The formation of PU films from PUDs is a multistep process, called casting technique. It starts when PUD is applied on a surface. At the beginning of this process, the dispersion contains 20-50 wt% solids content (Scheme 4c)). When water is evaporating, the PUD becomes more concentrated and the particles are closer to each other (Scheme 4d)). In this step, the particles are still round-shaped, which provides water penetration between them. Afterwards, when the particles modulus is exceeded by the drying forces, the soft PU nanoparticles deform to give mechanically weak void-free film (Scheme 4e)). The next phase consists of the coalescence of small particles being in a close contact, resulted in the disappearing boundaries between them (Scheme 4f)). Finally, due to the polymer inter-diffusion, the PU chains interpenetrate, providing the entanglements, which gives continuous and mechanically strong film.[81-84]

The individual steps of film formation are not always well defined and may occur at the same time. These stages depend on several factors. Firstly, a clear continuous film is obtained above the minimum film-forming temperature (MFT), at which the particles are possible to deform due to sufficient capillary force for the coalescence process. The MFT is related to T_g of PU and thereby the polymer softness. Below this temperature, water evaporation from PUDs leads to opaque and discontinuous materials. Another factor affecting the film-forming process is the PU particle size. It was found that large particles need short time for drying, however smaller particles produce stronger coatings with better penetration properties. Moreover, PUDs containing mixture of harder and softer particles lose water slower than PUDs consisting of uniform particles. Also low-viscous particles are desirable for obtaining of good materials.[74,81-83,85]

General properties of films obtained from PUDs are essentially the same like in solvent-borne PUs and depend on HS content, crosslinking density, SS-HS microphase

separation, etc. However, in the case of ionic PUDs, additional ionic centers affect HS crystallinity, PU thermal behavior and water sensitivity. The improvement of water resistance is limited due to the fact that decreasing amount of ionic groups, which reduces the films water swellability, is associated with simultaneous decreasing of PU stability. Therefore, optimization of the ionic centers concentration is an important step in design of PUDs and PUD-based films. Moreover, segregation of the ionic groups into macrodomains forms physical networks, improving properties of PU ionomers. Solvent resistance may be improved by crosslinking formation. This can be obtained in the reaction between water-dispersible groups and for instance carboimide or aziridine or by using of crosslikable sites. On the other hand, increasing of crosslinking density causes problems with the film formation because it leads to higher T_g and hence temperature for forming of PUD-based material. The films properties depend also on other factors, such as compatibility between ionic centers and PU backbone, the length of the spacer between the ionic groups and the polymer chain and the type of the neutralizing agent.[56,81,85,86]

1.5.4. Manufacturing processes of waterborne polyurethanes

There are several manufacturing processes of PUDs. In all of these methods the NCO-terminated low-molecular weight prepolymer is prepared in the first step. The differences between preparation techniques of PUDs are located in the chain extension stage.[9,56,87]

The oldest method for obtaining of PUDs is the acetone process. In this technique an organic solvent, such as methyl ethyl ketone, tetrahydrofuran, dioxane or preferably acetone is added to the prepolymer and chain extended in the next step. Acetone is the most commonly used due to its miscibility with water and low boiling temperature. The viscosity resulting after chain extension is controlled by a polar solvent, preventing the formation of hydrogen bonds between the PUs. The PUD is obtained by phase inversion after addition of water to the homogenous mixture and removing of an organic solvent. The advantages of this process are high reproducibility, formation of PUDs with small particle size and tight molecular weight distribution and high quality of obtained PUs. However, mostly linear PUs with molecular weight up to 100 000 are manufacturing by this method. Moreover, the acetone process is economically and environmentally unfavorable due to large amount of solvent used.[56,74,87-90]

In the prepolymer mixing process, the prepolymer being in a form of solution or melt, is directly emulsified with water. This technique is suitable for low-viscous prepolymers. However, the viscosity may be reduced by addition of small amount of solvent such as N-methyl pyrrolidyne. The dispersion step should be performed at low enough temperature to avoid reaction between –NCO groups and water, leading to formation of polyurea. Thus, low-reactive cycloaliphatic diisocyanates are mostly used in the prepolymer process. In the next step, PUs are chain extended by addition of di- or polyamines to the aqueous phase. Advantages of this method are simplicity, reduction of solvent amount, formation of PUs with higher molecular weight and more branched structures compared to the acetone process. On the other hand, the PU properties are inferior due to carrying out of the chain extension in a heterogeneous phase.[56,74,87,88]

In the melt dispersion method the NCO-terminated prepolymer reacts with an excess of urea or ammonia, giving the urea- or biuret-terminated prepolymer. In the next step, the obtained capped oligomer is dispersed in water. The reaction does not need any cosolvent, because the viscosity is controlled by high temperature of the reaction. After the self-dispersion, the chain extension is carried out by methylation of the oligomer biuret groups with formaldehyde at lower pH. Although this process is simple and substantially fast, it is not widely used in preparation of PU coatings.[56,63,74,90]

In the ketamine/ketazine technique, the prepolymer is homogeneously mixed with the blocked diamine (ketamine) or hydrazine (ketazine) and dispersed in water. The chain extension occurs as a result of simultaneous liberty of the amino function after hydrolysis and then spontaneous reaction with NCO-terminated prepolymer. PUDs prepared by this method are used for the production of high performance coatings.[9,56,74]

1.5.5. Applications of polyurethane water dispersions

PUDs have been recently applied in the area previously monopolized by conventional solvent-borne PUs and as adhesives and coatings for various surfaces. It was found that PUDs with larger particles are used when rapid drying of the surface coatings is preferred, whereas PUDs with smaller particles are applied when deep penetration of a PUD is desired.[56,91]

The main application of PUDs is coating industry. They can be classified as coatings for flexible surfaces, for finishing and for wood. The earliest and the widest area

of PUD applications are textile coatings. Proper PUDs give waterproof textile coatings with good water permeability, used widely for the production of leather substituents. Paper fibers treated with PUDs have improved strength and increased the tendency to ink to be absorbed into the paper rather than run on the surface. Since PUDs provide high abrasion resistance, high gloss and high fouling resistance, they are widely used for wood coatings. Plastic primers based on PUDs provide energy absorption and act as a buffer between the hard topcoat and the softer plastic substrate. PUDs also found applications as corrosion protection for metals due to increasing of toughness and wear resistance.[56,74,92,93]

Relatively new area for using of PUDs is biomedical industry. This field has received increasing interesting due to questing for elimination of the side effects caused by organic solvents in biomedical polymers. The advantages of PUDs are mechanical strength, biocompatibility and non-toxicity for bladder smooth muscle cells, fibroblasts and endothelial cells. Due to their properties, PUDs can be used for soft tissue engineering scaffolds, nanoparticles for drug delivery, treatment of ocular diseases and breast cancer. Moreover, PUDs are applied as antibacterial materials in wound healing.[5,94,95]

1.6. Polyurethane nanocomposites

Nanocomposites are polymer-matrix composites containing components with at least one dimension lower than 100 nm. This class of materials covers the group between organic polymers and inorganic glass. The role of fillers is enhancing of polymer properties, especially of polyurethanes. Technical and scientific literature report PU nanocomposites with nanoclays, silica, silver nanoparticles, cellulose, carbon nanotubes, titanium, polyaniline and other fillers. However, nanoclays and silica are the most common.[96-106]

Among layered aminosilicate clays, montrillomonite (bentonite) is widely used in PU nanocomposites. For these materials uniform dispersity of the clay nanolayers is more desired than their aggregation as tactoids. The nanolayer exfoliation leads to improving of mechanical, thermal and gas-barrier properties in comparison to the same PU with smectic clay or neat PUs. The degree of exfoliation can be increased by *in situ* polymerization, solution blending, melt blending, high shear mixing and several other methods.[97,98]

Among inorganic fillers, silica nanoparticles feature relatively low reflective index, high hardness and commercial availability. Due to silanol groups present on the silica surface, the nanoparticles may interact with HS and SS of PUs, giving improvement of the polymer materials. It was found that addition of silica to PU matrix leads to increasing of storage modulus in the rubbery region, tensile strength and elongation at break. PU-nanosilica nanocomposites can be prepared by blending method or *in situ* polymerization. The major disadvantage of these materials is tendency to the nanofiller agglomeration, stronger in the nanocomposites prepared by blending technique than *in situ* hydrolysis. This behavior is related to the fact that during *in situ* polymerization nanosilica particles are chemically bonded with PU, which prevents their aggregation. In contrast, in the blending method the possibility of chemical bond formation is very low, resulting in the nanofiller aggregation through hydrogen bonds. However, the nanocomposites obtained from blending method have higher microhardness than those prepared by *in situ* polymerization.[97,98,107]

1.7. Biostable and biodegradable polyurethanes.

Biostable versus biodegradable PUs are polymers with opposite properties belonging to the versatile class of PU materials. Traditional PUs have been used as biomaterials since the 1960's, typically for production of catheters, pacemaker leads, artificial heart prostheses and implants. These long-term biomedical devices require biostable PUs, because biodegradation comes with loosing of the material shape and mechanical properties. The PU biostability can be enhanced through modifications of SS substitutions by elimination of their reactive sites, mostly ester or ether groups. Therefore, polyether and polyester SSs have been substituted with polycarbonate, polybutadiene or polydimethylsiloxane. It has been investigated that polycarbonate SS is more stable than polyether SS. Another technique for improvement of oxidative cleavage resistance is the polymer endcapping with polydimethylsiloxane groups, which imparts the PU hydrophilicity. Moreover, increasing of the HS amount causes decreasing of the number of possible degradation sites, resulting in improved PU stability.[23,35,95,108,109]

Although PUs are widely applied in biomedical devices, toxic pre-cursors used for their synthesis may lead to release of carcinogenic substances inside the human body. Due to these problems, the interest in restorable and biodegradable PUs has been increasing in recent years. Biodegradable elastomeric PUs found applications as artificial

skin, nerve conduits, cardiovascular, short-term implants, cancellous bone graft substitutes and in oral drug administration. These polymers may be prepared by incorporation of hydrolysable groups into the PU backbone by several ways. The most common method is using of biodegradable polyester SS, such as poly(ε-caprolactone), poly(lactide), poly(glycolic acid) and their copolymers. Another way is using of diisocyanates derived from amino acids, which are non-toxic in comparison to traditional diisocyanates.[23,35,108,110,111]

2. Methods of characterization

The samples investigated in this work are polymer dispersions/solutions in water or in acetone. In this form they were measured by scattering techniques such as dynamic light scattering (DLS) and static light scattering (SLS) to obtain information about the particle size, dispersity, shape and molecular weight. Moreover, the particle size and shape were investigated also in the dry form, deposited on mica surface, by atomic force microscopy (AFM). After drying of the dispersions, continuous polymer films were formed. Their microstructure and mechanical properties were carried out by AFM, scanning electron microscopy (SEM), tensile test and dynamic mechanical thermal analysis (DMTA). The second part of this dissertation describes the morphology changes of PU elastomers before and after hydrolytic degradation tests, measured by AFM and SEM techniques.

Other methods of characterization, not described below in details, were also used for characterization of PUDs and PUD-based films. The formation of PU nanoparticles was monitored by Fourier transform infrared spectroscopy (FTIR), the thermal degradation of the films was investigated by thermogravimetric analysis (TG) and differential scanning calorimetry (DSC) and their water resistance was carried out by water uptake experiments.

2.1. Dynamic light scattering (DLS)

Dynamic (*quasielastic*) light scattering measures the intensity of the scattered light fluctuations, caused by the Brownian motions of the scattering particles. This method is a standard technique for determination of particle translational diffusion coefficient and thereby the equivalent spherical hydrodynamic radius (R_H). The main differences between DLS and SLS are investigating of the temporal structure by DLS instead of angular distributions in SLS and monitoring of the particle fluctuations over short time intervals in DLS in contrast to the averaged intensity measured by SLS.[112-114]

The principle of DLS is that the Brownian motion velocity depends on the particle size. In general, smaller particles diffuse faster than larger particles in a liquid medium, resulting in shorter timescale of fluctuations intensity for smaller particles. The particle Brownian motions for non-interacting monodisperse rigid spheres are defined by the

diffusion coefficient (D), which can be converted into the hydrodynamic radius of the particle (R_H) by the Stokes-Einstein equation:

$$R_H = \frac{k_B T}{6 \pi \eta D} \quad (1)$$

where k_B is the Boltzmann constant, T is the absolute temperature and η is the solution viscosity.[113-115]

2.1.1. Electrophoretic dynamic light scattering

Electrophoresis describes the interplay between the colloidal particle motions and electrical field formed by the particle charges under apply of an electric field. The electrophoretic mobility (μ_E) is related to zeta potential (ζ) by the Henry equation:

$$\mu_E = (\frac{2 \varepsilon \zeta}{3 \eta}) \, f(\kappa a) \quad (2)$$

where κa is the Henry function describing the ratio of the particle size to the double layer thickness and ε is dielectric constant. Measuring of the electrophoresis provides information about the physical stability of dispersed particles through investigation of repulsive electrostatic forces between them. Zeta potential is defined as a potential of the boundary between particle ions and solvent. In general, low values of ζ, typically between +30 mV and -30 mV, indicates the particle aggregation.[115,116]

2.2. Static light scattering (SLS)

Static (*elastic, Rayleigh*) light scattering investigates concentration and angular dependence of the scattered light intensity to yield the molecular mass and molecular size. In this method, the scattered light intensity is measured as voltage on photodiodes, expressed by the Rayleigh ratio (R_θ) as:

$$R_\theta = \frac{i_\theta r^2}{I_0} \quad (3)$$

where i_θ is the scattered beam intensity, I_0 is the incident beam intensity and r is a distance between scattering cell and detector.[112,117]

Determination of molecular weight in SLS is given by Zimm equation:

$$\frac{K\,c}{\Delta R_\theta} = \frac{1}{M_w}\left(1 + \frac{q^2 R_g}{3}\right) + 2A_2 c \quad (4)$$

where c is the concentration of macromolecules in solution M_w is the weight-average molecular weight, R_g is radius of gyration and A_2 is the second virial coefficient. After extrapolation of both $c \rightarrow 0$ and $\theta \rightarrow 0$, the new curves cross $K\,c/\Delta\,R_\theta$ at value $1/M_w$.[115,118]

2.3. Atomic force microscopy (AFM)

Atomic force microscopy (AFM), also called scanning force microscopy (SFM), is a basic method for all nanoscopic research. This technique is widely used for monitoring of PUs surface analysis due to possibility of detection the differences between HS and SS domains. The principle of AFM is measuring of the force between the investigated sample and the AFM tip.[119,120]

The central part of AFM instrument is the tip (probe) located on the flexible microcantilever. Commercially available tips and cantilevers are usually made from silicon nitride (Si_3N_4) or silicon (Si). Additionally, the cantilever is coated with a thin layer of gold or aluminum. The AFM probes are cylindrical canoe-shaped or four-sided pyramids with very flat faces. Cantilevers are usually either V-shaped or rectangular. During the AFM measuring, three regimes of forces between the tip and the sample can be distinguished: i) negligible force when the probe is far from the surface, ii) an attractive forces for closer distance, iii) very strong repulsive forces between the tip and the sample when they are very close to each other.[119-123]

The force between the probe and the sample is proportional to the cantilever deflection, acting as a spring. In most AFM instruments, the deflection is measured by applying a laser beam reflected from the top of the cantilever and directed to sensitive photodetector position, which enables monitoring of changes in the laser positions. During the imaging, the probe scanning over the sample is provided by a piezoelectric material, resulting in a topography map of the sample. The AFM instruments have limitations in a maximum scanning area, up to 200 μm × 200 μm for xy axis and up to 15 μm range for z axis (height).[119,120,122,124]

There are two general AFM imaging modes: i) static mode, recording the static cantilever deflection and ii) resonant mode, keeping constant amplitude of the cantilever

oscillation during the scanning. In contact mode technique, the tip reminds in a contact with the sample, while constant or variable force is applied. This method is often used for imaging of hard and smooth surfaces due to possibility of damage to soft samples. In tapping (intermediate) mode, the cantilever oscillates near the sample surface. During the measuring, the changes in the oscillatory amplitude give information about the sample topography and properties. The intermediate mode produces phase images, giving information about the sample adhesion, stiffness and viscosity. In this technique the sample interacts with the tip in lower degree than in the case of contact mode and is mostly used for imaging of soft biological samples. In non-contact mode, the cantilever is oscillating at much smaller amplitude than in tapping mode. The tip does not contact the sample, which results in lower image quality than in the intermediate method.[121,123]

2.4. Scanning electron microscopy (SEM)

Scanning electron microscope is the electron microscope, in which a beam of electrons is employed for scanning a sample to form a high-resolution 3-D image. SEM provides information about chemistry, crystallography and morphology, which makes it important method for microstructure characterization of various organic and inorganic materials from nanometer to micrometer scale.[125-127]

The area examined by SEM is irritated with a focused electron beam, generated by electron gun and controlled by series of lenses and apertures. The signals are inelastically scattered by the sample and collected as a function of the incident beam position. The interaction between the sample and the electron beam produce various types of signals, such as secondary electrons, backscattered electrons, x-rays, Augler electrons and cathodluminescence.[125-127]

The main advantage of SEM is that larger field of a measured sample can be imaged, compared to AFM. Thus, SEM provides general imaging of polymeric films in lower magnification and more detailed analysis in higher magnification. The magnification can be controlled by adjusting of the scanned area, changing of the working distance or varying of the accelerating voltage.[125]

2.5. Tensile test

Tensile testing is one of the most widely used short-term mechanical investigations of materials, due to easy to perform measuring giving reproducible results.

This method provides information about tensile strength, elongation and modulus. During the experiment, deformation and elongation of the tensile specimen at standard cross head speed is registered as the diagram of tensile force versus tensile elongation.[128-130]

Tensile test allows investigating of elastic and plastic deformation of solid materials. Elastic deformation is a result of bonds relaxation and returning of the material to its original shape after removed of a small stress. Application of higher stress causes plastic deformation, not recovered after the stress removal. The initial part of the stress-strain curve is linear for most materials. This part is called Young's modulus or elastic modulus. As a result of stress rising, the elastic limit of the material and onset of the plastic behavior is defined by yield strength.[129,130]

2.6. Dynamic mechanical thermal analysis (DMTA)

DMTA provides information about the viscoelastic behavior of materials, by analyzing of the sample response to applied oscillating force. Elasticity is attributed to solid materials, whereas viscosity to fluids. Polymers behave in a dual manner, displaying the balance between viscous flow and elastic recovery with time and with temperature. The behavior in solid state is reflected to impact resistance and stress and creep relaxation, whereas viscoelasticity gives information about crosslinking, molecular weight and thermal stability.[131-133]

During DMTA experiment, a periodic stress is applied and the resulted behavior between in-phase and out-of-phase stress and strain is registered. The angle, by which the stress and strain are out of phase, is called delta (δ). Highly elastic materials are described by small phase angle, whereas large values of δ are typical for highly viscous materials. The stress measured by DMTA is used to calculate the storage modulus (E') and the loss modulus (E''), which in a shear mode are replaced by G' and G''. In general, G' describes elastic properties of a sample and G'' reflects the loss of energy during the friction and polymer chains motion. The ratio E'/E'' or G'/G'' is used for calculation of tan δ, which provides information about α and β relaxations. The α transition (T_α) is related to T_g, assigned to the main chains movement, whereas β transition (T_β) occurs at lower temperature and is assigned to other molecular motions. Crosslinked polymers are characterized by increasing of tan α and G' with increasing of crosslinking density.[131,132,134]

3. Aims of the Thesis

The main objective of this dissertation is preparation and characterization of polyurethane (PU) films formed after drying of polyurethane water dispersions (PUDs) based on polycarbonate macrodiol (PCD).

The reason for a great interest in waterborne polyurethanes is elimination of volatile organic compounds and hazardous air pollutants evaporation to the atmosphere, inevitable in the production of solvent-borne PUs. Incorporation of hydrophilic groups, providing dispersity in water, deteriorates PUD-based film properties. Therefore, PUDs need to be modified to obtain materials comparable to traditional solvent-based PUs.

In the present study, we focus on optimization of the HS and SS ratio leading to a proper balance between hydrophilicity and hydrophobicity of the PUDs. The novelty of the firstly synthetized PUDs is that they are based on linear solely aliphatic components, leading to thermoplastic PUD-based films after water evaporation from the dispersions. Thus, beside the fact that the PUs are prepared by environmentally friendly technique, they can be re-processed. The thermoplasts are further improved by blending of the PUDs with two types of colloidal silica, giving the nanocomposite films. Finally, we modify the acetone process of PUDs preparation by elimination of any commercial chain extender addition and by using of water both as a dispersity medium and for crosslinking of PUs. As a result we obtain cheaper, simpler and more ecofriendly technique for PUDs synthesis. This part of the Theses is described in details in Appendices I-IV.

The additional part of this work is aimed for hydrolytic stability and degradation study of aliphatic PU elastomers, tested under conditions mimicking the physiological environment. The stable PU films are prepared from traditional linear components, whereas the degradable PUs incorporate additionally the degradable unit D,L-lactide-based oligomeric diol (DLL) in their backbone. The first class of PUs can be used for example as durable topcoat, while degradable PUs are promising short-term materials. The analysis of the stability/degradation is focused mostly on the morphology investigation carried out by macroscopic techniques. The extended discussion of this part can be found in Appendices V and VI.

4. Results and discusion

4.1. Materials and preparation conditions

PUs included in this Thesis were prepared from linear solely aliphatic components. In the all cases HDI and PCD were used for the synthesis.

The main part of this work is focused on PUDs and PUD-based films. All PUDs were based on PCD T4672 (for detailed structure see Scheme 5) building SSs, neutralizing agent TEA and DMPA providing water solubility. The control of the mixture viscosity was done by addition of acetone. The same reaction conditions, such as the rate of mixing, the reaction time, temperature and the solid content in acetone and in water were kept for all PUDs. Moreover, the PUD-based films were prepared by the same casting method and dried at the same temperature and by the same period of time.

The dispersions were modified by various ways. At first, BD was used as a chain extender, to obtain thermoplastic PUD-based films. The PUDs were further improved by addition of commercial colloidal silica Ludox TMA or Ludox AS, leading to thermoplastic nanocomposite films. Finally, the acetone process was modified by elimination of the chain extension step. For this purpose 1.05 NCO exceed was used for linear system, whereas 1.5 NCO exceed led to water-crosslinking PU nanoparticles.

The second part of this dissertation describes aliphatic PU elastomers tested for hydrolytic degradation under conditions mimicking human body. The hydrolytically stable PUs were prepared from HDI, BD and PCD. The elastomers unstable in the physiological environment contained in their structure also DLL, accelerating the hydrolytic degradation. The reaction conditions and films preparation were the same in the all cases.

4.2. Waterborne polyurethanes and PUD-based films

4.2.1. Waterborne thermoplastic polyurethanes

The paper I is focused on synthesis and analysis of PUDs based on polycarbonate macrodiol. The innovation of this study was using of BD as a chain extender for this type of PUDs, leading to formation of TPU films. The PU nanoparticles dispersed in aqueous

medium were characterized by DLS, whereas dried continuous films were tested for morphology, mechanical, thermal and water resistance.

The preparation of PUDs included using of acetone for reduction of the mixture viscosity and elimination of the mixing problems. For this purpose the classical acetone process was slightly modified by reversed neutralization step with the chain extension. The first type of prepared PUDs incorporated in the PU backbone three bifunctional compounds containing hydroxy groups: DMPA, BD and PCD. Moreover, linear aliphatic diisocyanate HDI was used to obtain linear polymers. The steps of the reaction are shown in Schema 5. The modification of the PUD properties was given by changing of the OH-terminated monomer molar ratio, while keeping constant the isocyanate index ($[NCO]:[OH]_{total}$ = 1.05). The reason of using small NCO excess (1.05) was to recompense the reaction between HDI and water present in components, air and so on, thus it led to solely linear PUs. The PUD-based films were prepared by casting of the PUDs in Teflon molds.

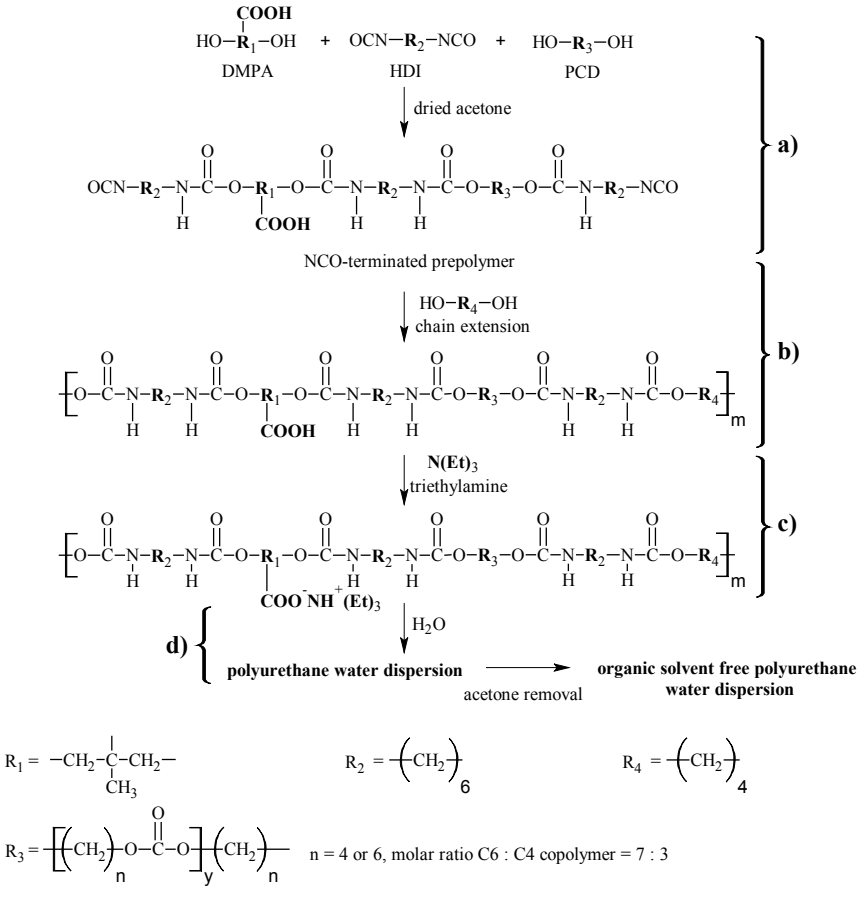

Scheme 5. Preparation of PUDs: a) pre-polymer formation, b) chain extension, c) neutralization, d) water dispersion.

4.2.1.1. Particle size and stability

The initial analysis of the PUDs concerned investigation of the PU nanoparticles dispersed in water (see Fig. 3). It was found that the particle size decreases with increasing of DMPA amount, because of increasing of the ionic groups number and therefore the electrostatic repulsion forces. Additionally, the particle size is affected in a minor extent also by BD amount. The higher BD concentration, the larger particles are formed, due to increasing of the PU chain stiffness.

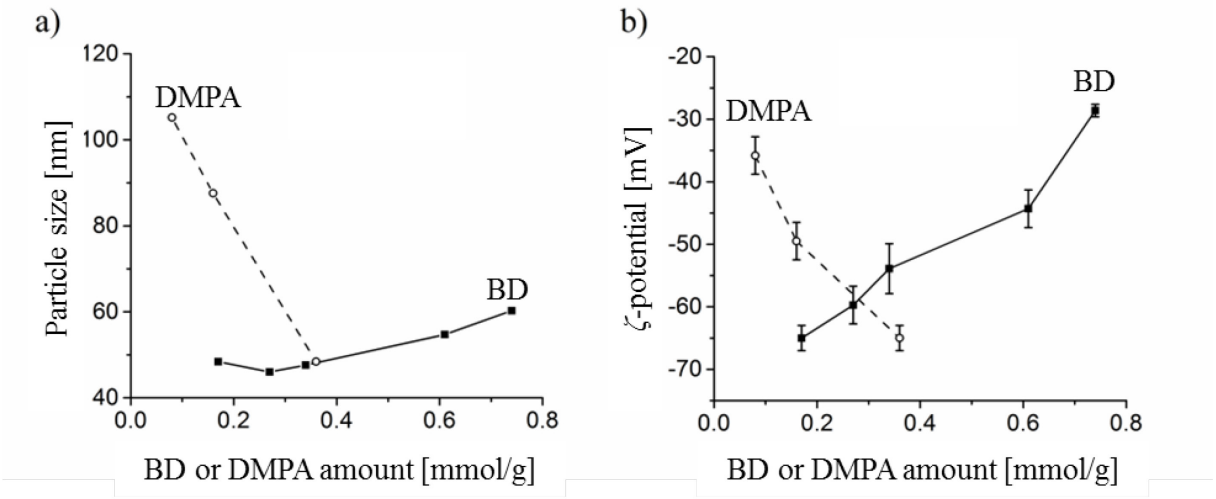

Figure 3. Characterization of PU nanoparticles in water: a) particle size, b) ζ-potential, as a function of BD and DMPA concentration.

Since the PUDs contain pendant COO^- groups, they are anionomers characterized by negative values of ζ-potential. Increasing of DMPA amount causes not only decreasing of the particle size, but also decreasing of ζ-potential. This behavior can be explained by higher ratio of the particle electrical double layer to their volume for smaller particles. In contrast, increasing of BD concentration leads to less stable dispersions with bigger particles. However, all prepared PUDs were stable minimum for one year.

4.2.1.2. Film properties

The first investigation of PUD-based films was carried out by AFM in order to find a proper method for the films preparation. For that reason, the same PUD was dried at different temperatures (Fig. 4). The phase images revealed only slight microphase separation between HS and SS for fast water evaporation (Fig. 4a)). This sample was heated at 50 °C directly after casting on a Teflon plate. Therefore, HSs did not have

enough time for self-organization, which resulted in a film with poor properties. During the second method, the PUD was slowly dried at ambient temperature, leading to randomly oriented rod-like structures (Fig. 4b)) and improvement of the sample properties compared to the first technique. The last modification combined slow water evaporation at room temperature, followed by heating at 50 °C (Fig. 4c)). Casting well above T_g provided high mobility of the polymer chains, resulted in the regular arrangement of HSs and thus the strongest films. The comparison of these three methods allowed choosing the last one for preparation of all PUD-based films, presented in the papers I-IV.

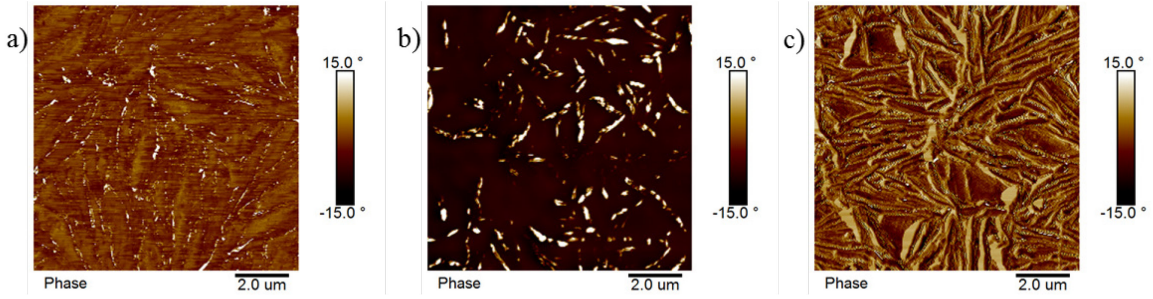

Figure 4. AFM phase images of PUD-based films prepared by drying: a) at 50 °C directly after casting of the PUD, b) at ambient temperature, c) at room temperature followed by drying at 50 °C.

The detailed morphology of the PUD-based films was carried out by two microscopic techniques: AFM and SEM. The both methods showed similar results of the same sample (Fig. 5). This means that fibril-like structure of the films surface observed by AFM is confirmed by SEM. The width of the fibrils between 80 and 120 nm and the hollow dips were visible in the both images, confirming that AFM and SEM are proper for investigation of the PUD-based film microstructures.

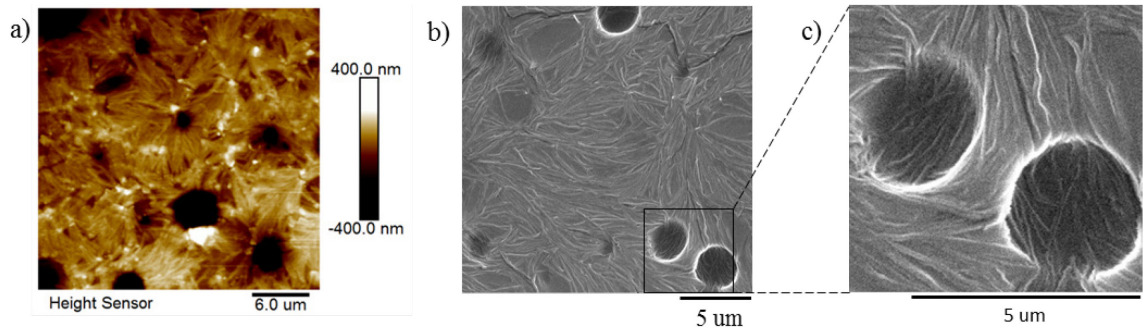

Figure 5. The microstructure of a PUD-based film: a) AFM Height image, b) SEM micrograph in lower magnification, c) SEM image of marked area in higher magnification.

The thermal behavior of obtained PUD-based films was investigated by DSC. It was found, that all samples have the same value of T_g, around -34 °C, indicating similar degree of phase separation. Moreover, the analysis of the peaks related to relaxation of SSs and melting of HSs leads to conclusion that the motion of SSs is not significantly affected by the physical crosslinks. However, the chain motions and crystallization of PCD are hindered by the ionic groups of DMPA. Therefore, it can be assumed that the ionic species have greater influence on SSs crystallization than HSs formed from BD and HDI.

The water uptake of the PU films was investigated by immersing of the samples in water and monitoring of the mass changes in time. The antagonistic influence of DMPA compared to BD on the water resistivity was noticed. The sample containing the highest BD amount was characterized by 7 wt% of water uptake, whereas the highest DMPA concentration resulted in 115 wt% degree of swelling. Deterioration of the water resistance caused by increasing of DMPA amount is a result of the ionic groups formation. On the other hand, in spite of the polar nature of BD, it reduces the water uptake (from 58 wt% for the lowest concentration to 8.5 wt% for the highest amount of BD), due to creation of HSs inhibiting water penetration into the films.

The effect of HS concentration on the surface appearance was monitored by SEM analysis (Fig. 6). The most homogenous structure was observed for the sample containing the lowest BD concentration (Fig. 6a)), whereas the tendency to creation of hollow dips was increasing with increasing of BD amount. The comparison of the SEM and water uptake results revealed that the pores do not deteriorate the water resistance. Furthermore, the most hydrophobic film, containing the highest BD concentration was characterized by

the highest number of the hollow dips. This suggests that in this case water evaporation during the film formation was the most difficult, resulted in the most pores structure.

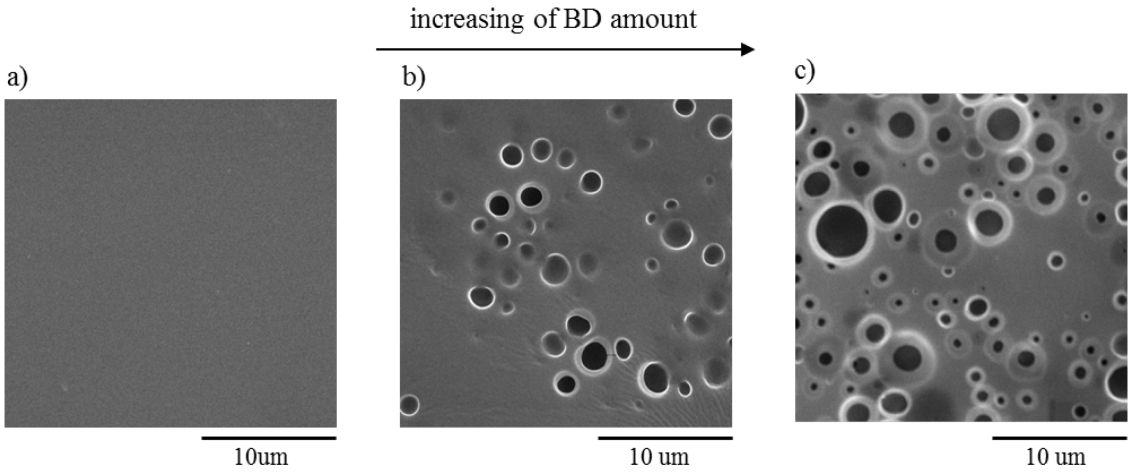

Figure 6. SEM images of PUD-based films containing various BD concentrations: a) 0.17 mmol · g^{-1}, b) 0.34 mmol · g^{-1}, c) 0.61 mmol · g^{-1}.

Tensile testing showed that BD improves mechanical properties of the PUD-based films significantly (Fig. 7a)). Increasing of BD amount causes increasing of Young's modulus (E) and tensile strength (σ_b), due to increasing of HS concentration. Moreover, improvement of elongation at break (ε_b) is a result of increasing of physical crosslinking density. In the case of DMPA (Fig. 7b)), the influence on ε_b was similar to the effect of BD, due to formation of higher number of hydrogen bonds. However, σ_b and E showed deterioration with increasing of DMPA amount, caused by negative influence of the ionic groups.

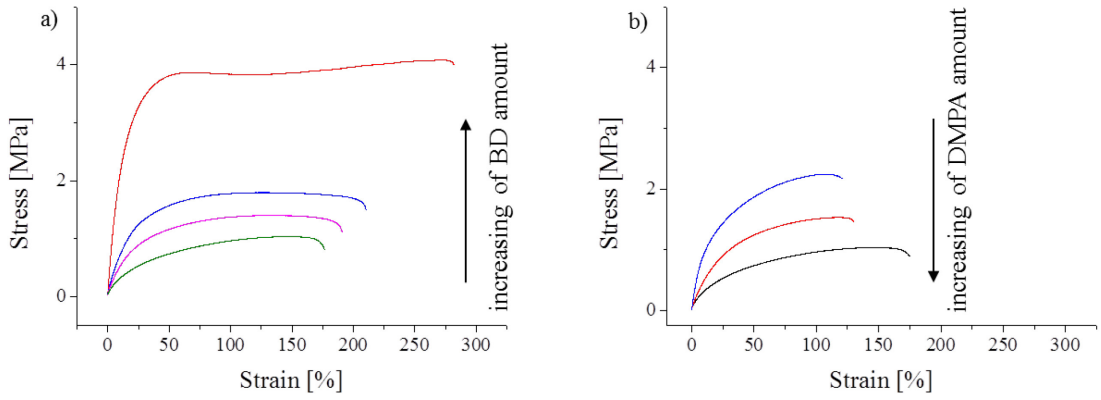

Figure 7. Tensile test curves of PUD-based films containing: a) various BD amount, b) various DMPA amount.

To assume this chapter, in the paper I waterborne PUs based on linear monomers were prepared. This led to formation of thermoplastic films based only on physical networks, soluble in organic solvents and possible to recycling. In this study, the influence of BD and DMPA was extensively investigated. It was found that BD being the main part of HSs, only slightly influences the particle size in water, but causes deterioration of the PUDs stability. Regarding to the film properties, BD improves the water resistance despite of promoting of the films porosity. The stronger impact of BD was observed as the significant improvement of mechanical properties, due to increasing of HS amount and physical crosslinking density. The ionic species, provided by DMPA, contribute to smaller PU nanoparticles and their better stability in water. However, their negative influence in the films resistance was noticed. It was observed, that increasing of DMPA amount leads to more water sensitive and mechanically weaker films. In summary, the PU nanoparticles dispersed in aqueous medium prefer high amount of DMPA, whereas the best PUD-based films are obtained with the highest concentration of BD. Thus, a proper balance between these two components is an important step in the PUDs designing.

4.2.2. Organic-inorganic PUD-colloidal silica nanocomposites.

The papers II and III are focused on investigation of the thermoplastic PUD-based films improvement. For this purpose, one PUD prepared in the first study (paper I) was used as organic matrix. The chosen dispersion was characterized by the narrowest size dispersity index, which means that it had the most homogenous particles among all PUDs obtained in the paper I.

The aim of organic-inorganic nanocomposite preparation was improvement of the PU films with simultaneous preserving of their thermoplastic character and thus their reusing and recycling. Colloidal silica aqueous sol was used as inorganic nanofiller and simply mixed with the PUD, forming new hydrogen bonds between the silica particles and the polymer matrix.

4.2.2.1. Characterization of the colloidal silica nanofillers

Two types of commercially available colloidal silica: Ludox TMA and Ludox AS were used for preparation of the nanocomposites. The both nanofillers were in a form of stable water dispersion. The main difference between them, provided by the

manufacturer, was used counterions: Na^+ for Ludox TMA and NH_4^+ for Ludox AS. The nanofiller particle size measured by DLS was similar in the both cases, around 35 nm. However, the main contrast between TMA and AS was the most visible after drying and AFM measuring (Fig. 8). It was found, that the dried nanofillers differ significantly in size and shape. The oval-shaped TMA particles in the size from 22 to 54 nm were observed (Fig. 8a)), whereas AS nanosilica was characterized by smaller (22-25 nm) and more homogenous hexagonal particles, forming honeycomb structure (Fig. 8b)).

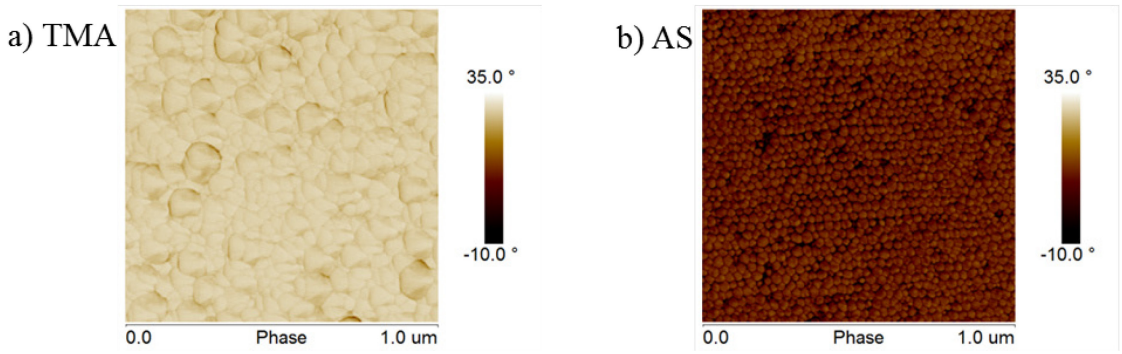

Figure 8. AFM phase images of dried colloidal silica: a) Ludox TMA, b) Ludox AS.

4.2.2.2. Investigation of a proper silica concentration in PUDs

The initial study of the nanocomposites was aimed to find a proper concentration of colloidal silica to obtain the best improvement of the PUD-based films. For this purpose, the PUD with 32 wt% of solid content was mixed with various concentrations of Ludox TMA to obtain the nanocomposites containing from 5 to 60 wt% of the nanofiller. The films were prepared by the same technique as in the paper I, to form the nanocomposite materials. The main advantage of this method was, beside the simplicity, the same aqueous medium, in which both silica and PU nanoparticles were dispersed. The preparation of the nanocomposites is illustrated in Scheme 5. Apart from the fact that the neat PU forms hydrogen bonds (Scheme 5a) and b)), incorporation of the silica nanoparticles between the polymer chains leads to formation of new physical crosslinks (Scheme 5c)). The films contained various concentrations of Ludox TMA were classified to three groups: 1) PU filled with the nanofiller with up to 10 wt% of TMA, 2) bicontionus intermediate systems composed of 25 and 32 wt% of silica and 3) silica matrix filled with the polymer contained 50 and 60 wt% of TMA.

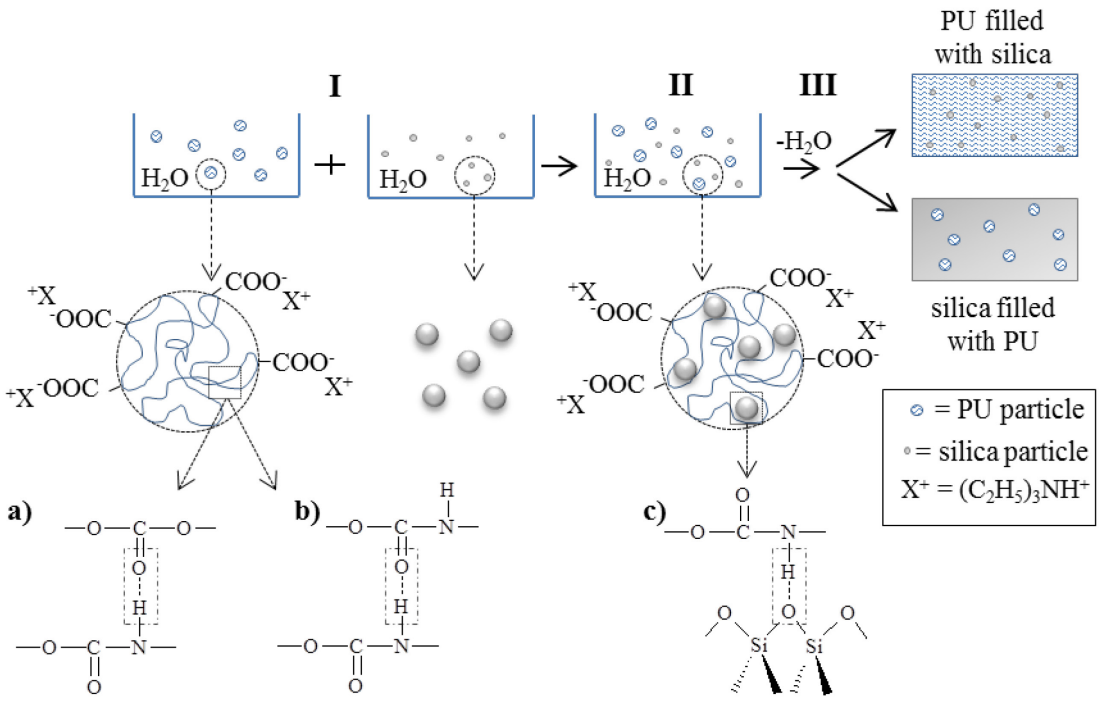

Schema 6. Preparation of PUD-colloidal silica nanocomposites: I) blending of PU and colloidal silica water dispersions, II) incorporation of silica particles between the polymer chains, III) formation of the nanocomposite films (various types depending on the nanofiller amount). Possibilities of H-bonding: a) urethane-carbonate groups (HS-SS), b) urethane groups (HS-HS), c) silica-urethane groups.

The nanocomposite films analysis started from evaluation of mechanical and thermal properties. Tensile test results revealed elastomeric-like behavior of the neat matrix and films with up to 10 wt% of Ludox TMA (Fig. 9a)). Moreover, slight improvement of the mechanical resistance was observed after addition of 5 or 10 wt% of the nanofiller, due to effective stress transfer from the soft PU to rigid silica particles. Higher nanofiller loading (25 and 32 wt%) resulted in more plastic behavior, caused by higher silica aggregation and thus lower energy dissipation. The films belonging to the last group were hard and fragile ceramic-like materials (Fig. 9b)).

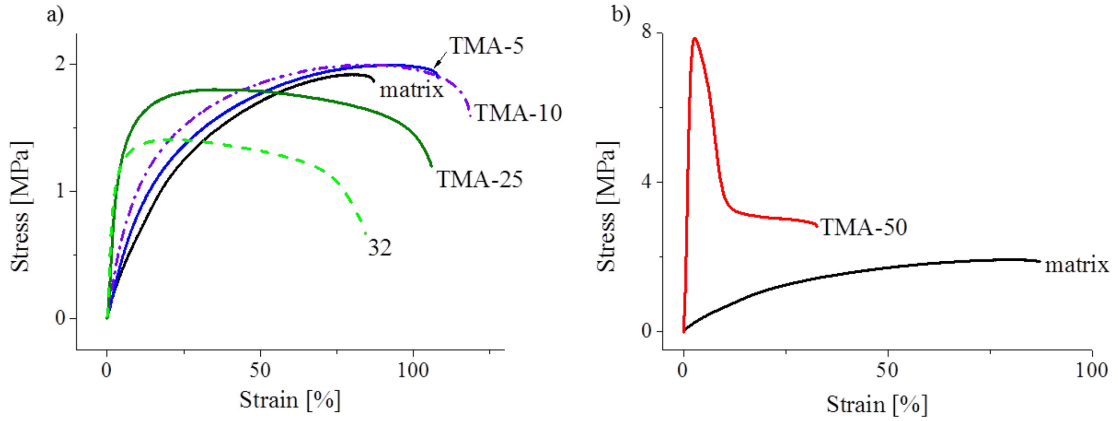

Figure 9. Stress-strain curves of neat PU matrix and: a) the nanocomposites containing up to 32 wt% of Ludox TMA, b) film with 50 wt% of the silica loading.

The viscoelastic properties of the PUD-colloidal silica nanocomposites were investigated by DMTA analysis (Fig. 10). It was found that increasing of Ludox TMA concentration increases *G*' values in the rubbery plateau region (Fig. 10a)), indicating that silica acts as a physical crosslinker. Melting of all samples and increasing of their T_m after addition of the nanofiller was observed as well. This means that Ludox TMA improves thermal resistance of the PUD-based films, with preserving their thermoplastic character. The lack of chemical reaction between the polymer matrix and the nanofiller was confirmed also by the same T_g for all samples, evaluated from the maxima of tan δ curves (Fig. 10b)). Moreover, the tan δ versus temperature dependence showed the blocking effect of silica particles on the PU chains mobility, resulted in the chains releasing at higher temperatures.

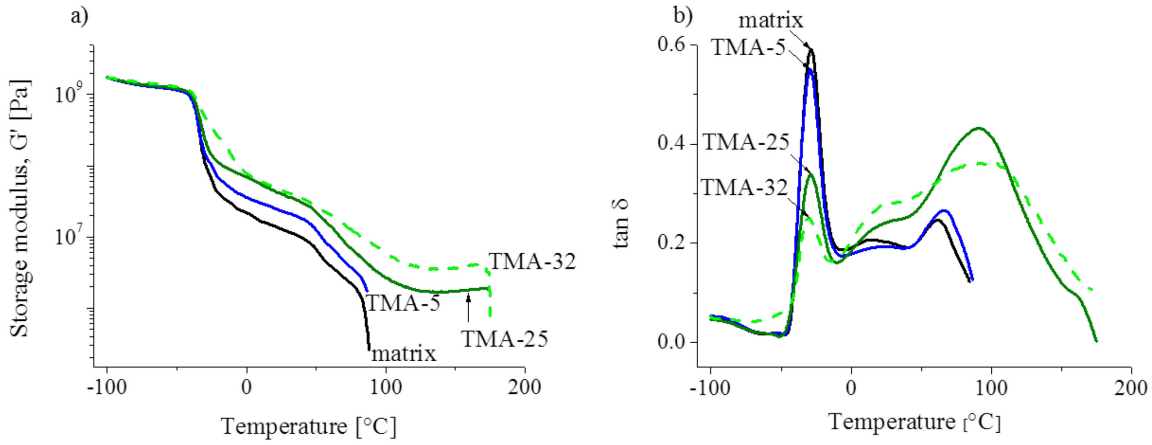

Figure 10. The temperature versus: a) storage modulus *G*', b) tan δ of the films containing various concentrations of Ludox TMA.

The influence of Ludox TMA on the films thermal resistance was confirmed also by TG. Shifting of the TG curves to higher temperatures proved that the films with growing content of silica need higher temperature to decompose. Thus, due to the nanofiller shielding effect, it acts as a mass transport barrier for volatile products. The TG thermograms also confirmed that the residues after the measurements were precisely equal to concentration of silica used for each nanocomposite, indicating that all organic part has been volatized during the analysis.

The morphology of PUD-based films containing various amount of Ludox TMA was investigated by SEM, AFM and optical microscopy. The most visible differences between the sample appearances were visible while comparing the nanocomposites containing 5, 32 and 50 wt% of the nanofiller.

The surface microstructure was monitored by combination of SEM and AFM (Fig. 11). Moreover, the roughness of the films was evaluated by AFM. The results obtained by the both microscopic methods were very similar, confirming each other. It was observed, that fibril-like matrix structure becomes smoother after addition of 5 wt% of TMA (Fig. 11a) and b)). It was a result of incorporation of small silica nanoparticles between PU chains. Increasing of the nanofiller loading caused rougher surface and separation of the rods (Fig. 11c)). This behavior was a result of high blocking of the polymer chains by Ludox TMA. This disordering was also visible in tan δ curves (Fig. 10b)) and as a deterioration of mechanical properties measured by tensile test (Fig. 9a)). The nanocomposite filled with 50 wt% of the nanofiller showed highly porous structure (Fig. 11d)), characteristic for ceramic materials.

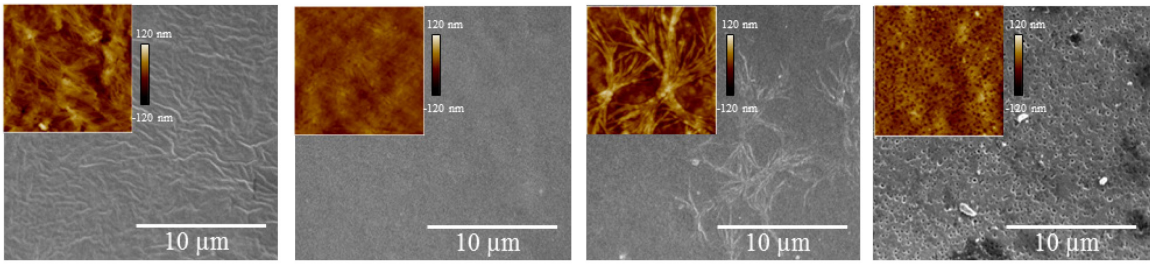

a) matrix b) TMA-5 c) TMA-32 d) TMA-50

Figure 11. The surface SEM and AFM (upper left corner) analysis of: a) neat PU matrix, b) nanocomposites with 5 wt % Ludox TMA, c) 32 wt% TMA, d) 50 wt% TMA. The scale 10 µm refers both to SEM and AFM images.

AFM was found to be a proper method for investigation of the nanofiller dispersity in the polymer matrix. For this purpose, the samples were broken in liquid nitrogen and the cross-section analyses were evaluated by phase images (Fig. 12), where PU matrix appears dark, whereas silica nanoparticles are visible as bright spots. Quite well dispersity of TMA, with PU layer separating the particles from each other, was observed for samples containing up to 32 wt% of the nanofiller (Fig. 12a) and b)). The morphology explained polymer-like behavior of these films, measured by tensile test (Fig. 9a)). This means that in the cases of the nanocomposites filled with maximum 32 wt% of Ludox TMA, the blocking effect of the silica particles is not strong enough to dominate over the PU matrix influence. However, the sample containing 50 wt% of the nanofiller shows high aggregation of silica with only small areas of dark fields corresponding to the polymer (Fig. 12c)). This microstructure is another confirmation for the ceramic-like mechanical properties of this film (Fig. 9c)).

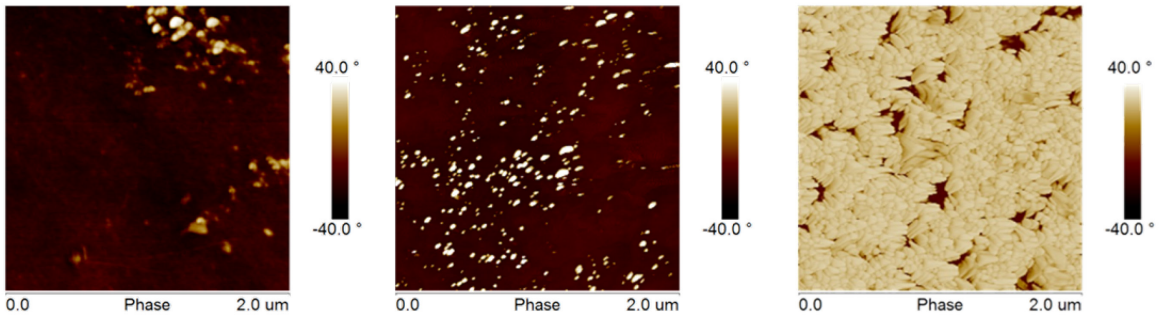

a) TMA-5 b) TMA-32 c) TMA-50

Figure 12. Cross-section AFM images of the PUD-based films containing various amount of Ludox TMA: a) 5 wt%, b) 32 wt%, c) 50 wt%.

The general sample appearances, measured by optical microscopy, find these explanations in the SEM and AFM results, as well. It was observed that the neat PUD-based film is transparent, whereas increasing of silica concentration leads to increasing of the samples opalescence. This phenomenon was caused by formation of silica aggregates and increasing of the films porosity, resulted in changes of the light scattering from the nanocomposites.

The last analysis of the PUD-based films containing six different concentrations of colloidal silica Ludox TMA was carried out for the water resistance. The water uptake of the PU matrix corresponds to DMPA incorporated in the PU backbone. The experiments

revealed that despite the fact that colloidal silica has hydrophilic nature, the addition of 5 or 10 wt% of the nanofiller leads to decreasing of the nanocomposite water swelling. This can be understood as less vacates possible for water molecules penetration, already occupied by silica nanoparticles. Further increasing of Ludox TMA concentration led to decreasing of the nanocomposite water resistance. This behavior was caused by increasing of hydrophilic silica influence and creation of porous films, facilitating water accommodation in their structure.

To summarize, in the paper II several samples including the neat PUD-based film and the nanocomposites with various concentrations of colloidal silica Ludox TMA, were compared. It was found that the samples can be classified in three groups containing PU matrix filled with silica, the intermediate materials and silica matrix filled with PU. The comparison allows concluding that increasing of TMA amount leads to variation in the sample properties, from elastomeric-like to ceramic-like. The best improvement of the PU films was noticed after addition of up to 10 wt% of silica. The most visible differences between the nanocomposites were observed while comparing films with 5, 32 and 50 wt% of the nano-filler loading, representing one sample from each group. The finding of the silica amount, proper for comparison its influence on the PUD-based films was useful in the paper III, focused on investigation of colloidal silica type on the PU samples.

4.2.2.3. The influence of colloidal silica type on PUD-based films.

In the paper III, two types of colloidal silica, Ludox TMA and Ludox AS, were used for preparation of the nanocomposites. It was expected, that Ludox AS will provide better improvement of the samples due to its smaller particles and thus higher possibility for formation of physical crosslinking with PU matrix. Basing on the information obtained in the paper II, the nanocomposites containing 5, 32 and 50 wt% of Ludox TMA and Ludox AS were prepared by the same technique and compared.

The surface SEM and AFM analyses showed that addition of 5 wt% of TMA smoothes the film in the higher degree than incorporation of 5 wt% of AS. It can be explained by slightly lower influence of colloidal silica Ludox AS containing smaller particles on the PUD-based samples. This lower impact was more desired in higher silica loading. The comparison of the nanocomposites containing 32 wt% of the nanofiller revealed that addition of Ludox AS does not perturb the PU matrix enough to deteriorate its fibril-like morphology. In contrast, using of Ludox TMA in this case leads to separated

fibrils. Thus, it can be concluded that silica AS is more compatible with the PU matrix than TMA. The nanocomposites with 50 wt% of the nanofiller loading showed protruding of silica particles above the films surfaces in the both samples. Moreover, the film containing Ludox AS revealed highly rough structure, whereas using of Ludox TMA led to high porosity.

The cross-section analysis of the nanocomposites showed similar results for silica loading up to 32 wt%. The significant difference was observed in the films containing 50 wt% of the nanofiller (Fig. 13). The sample with Ludox AS was characterized by highly packed silica particles and very small amount of PU between them (Fig. 13a)). For comparison, in the case of using TMA, despite the fact that the nanofiller forms high aggregates, the polymer matrix possess higher areas (Fig. 13b)). This observation suggests that PU chains are blocked in lower degree by TMA than AS in the cases of the highest silica concentration.

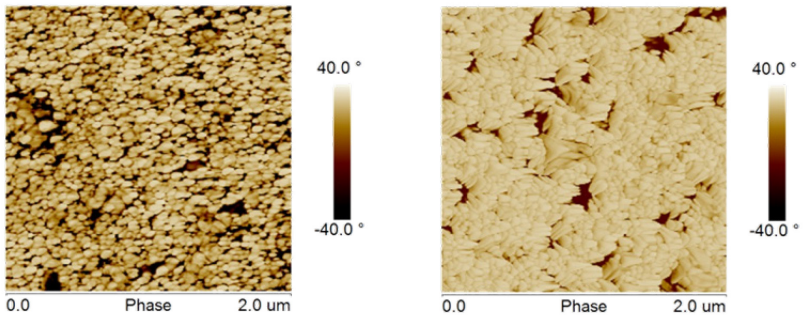

a) AS-50 b) TMA-50

Figure 13. Cross-section AFM phase images of the nanocomposites containing 50 wt% of: a) Ludox AS, b) Ludox TMA.

The comparison of static mechanical properties for the nanocomposites filled with two silica types showed significant differences after adding of 32 or 50 wt% of the nanofillers (Fig. 14). The slightly better improvement of fracture strain after addition of 5 wt% silica was observed while using Ludox AS than Ludox TMA, due to larger contact area between PU matrix and smaller AS particles, enabling higher physical crosslinking density. The significant enhancement of the film containing 32 wt% AS (Fig. 14a)) was caused by its unperturbed fibril-like structure characteristic for the matrix. In contrast, the deterioration of mechanical properties in the sample with 32 wt% TMA was a result of too high blocking of PU chains by the silica particles, resulting in separated rods (Fig.

11c)). Both samples filled with 50 wt% of the nanofiller were brittle materials (Fig. 14b)). However, the film containing Ludox AS revealed more ceramic-like features, whereas the nanocomposite with Ludox TMA was characterized by more plastic nature. This can be explained by their morphology. The sample with 50 wt% of TMA creates bigger agglomerates and larger matrix areas, sufficient to influence of the film properties.

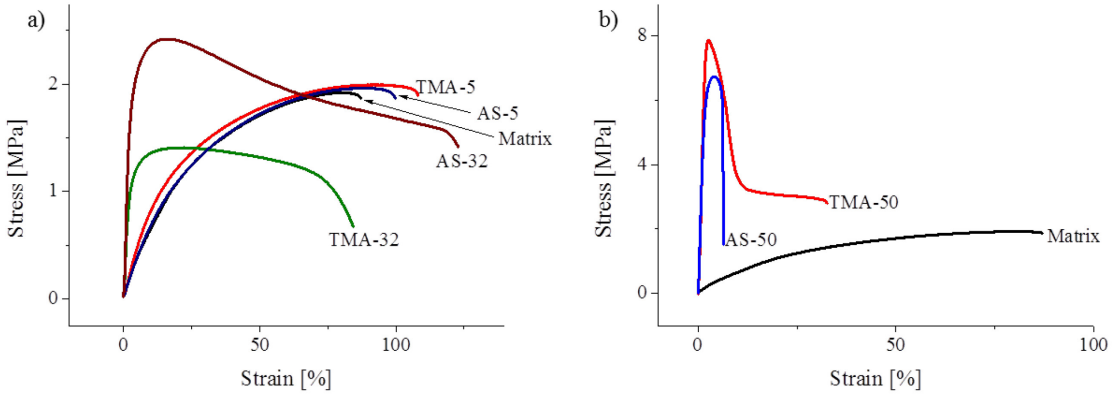

Figure 14. Stress-strain curves of neat PU and the nanocomposites containing: a) up to 32 wt% of silica, b) 50 wt% of the nanofiller.

The DMTA analysis confirmed that both silica types act as physical crosslinkers and the all nanocomposites are thermoplastic materials. The thermal resistance of the films was detected from *G'* versus temperature curves as increasing of T_m and from TG analysis as shifting of degradation steps to higher temperatures. The both techniques revealed more significant influence of Ludox AS than Ludox TMA, confirming its better compatibility with the PU matrix. This conclusion was confirmed also by water uptake experiments. It was fond that the best improvement of water resistance revealed sample containing 5 wt% of AS, indicating the best balance between its hydrophilicity and creation of new hydrogen bonds with PU.

To assume the paper III, in this study the representatives from each nanocomposite group, created in the paper II, were used to compare the influence of Ludox TMA and Ludox AS on the thermoplastic PUD-based films. It was concluded that Ludox AS containing smaller and more regular particles creates higher physical crosslinking density with the PU matrix than Ludox TMA. As a result, the nanocomposites with AS show better improvement of mechanical, thermal and water resistance than while using TMA. Therefore, nanosilica with smaller particles is more compatible with the polymer matrix.

4.2.3. Water-crosslinked polyurethane water dispersions without chain extender

The further improvement of PUDs based on polycarbonate macrodiol was described in the paper IV. In this study, waterborne polyurethanes leading to mechanically strong films were prepared without any commercial chain extender and crosslinked by water. In this paper, the self-assembly of PU chains/nanoparticles in two steps of the synthesis was monitored.

4.2.3.1. Modification of the acetone process

The PUDs were synthetized via modified acetone process. In this new technique the chain extension step (Scheme 5b)) was eliminated. This innovation led to reduction of the reaction time, manufacturing costs and toxicity.

Different DMPA:PCD molar ratios were used for control of the HS and SS amount. Moreover, the ratio [NCO]:$[OH]_{total}$ (isocyanate index) was set either 1.05 or 1.5. The small amount of NCO excess (1.05) was used for recompense of inevitable reaction between HDI and water present in the environment, thus led to linear PUs, whereas 1.5 NCO excess formed water-crosslinked systems. The self-assembly of PUs was investigated in two reaction steps: 1) after PU formation in acetone and neutralization of COOH groups (Scheme 5b)); and 2) final PUDs after acetone removal (Scheme 5d)).

4.2.3.2. Self-assembly study of PU nanoparticles

The initial monitoring of PU formation was carried out by FTIR. At first, the PU nanoparticles in acetone solutions/dispersions containing 1.05 (Fig. 15a)) or 1.5 (Fig. 15b)) NCO excess were monitored. The obtained spectra in the area of carbonyl stretching were similar in the both cases, indicating that in this step urea (band A) and urethane (band B and C) are formed in the reaction between HDI and water present in the solvent, components and air. Moreover, in the region attributed to the occurrence of isocyanate groups, the weak peak was observed only for samples containing 1.5 NCO excess, suggesting partial crosslinking via formation of allophanates, resulted from the reaction between isocyanate and urethane groups. In contrast, no NCO peak was detected for series with 1.05 NCO excess, indicating full isocyanate conversion to linear PUs chain extended by urea formation.

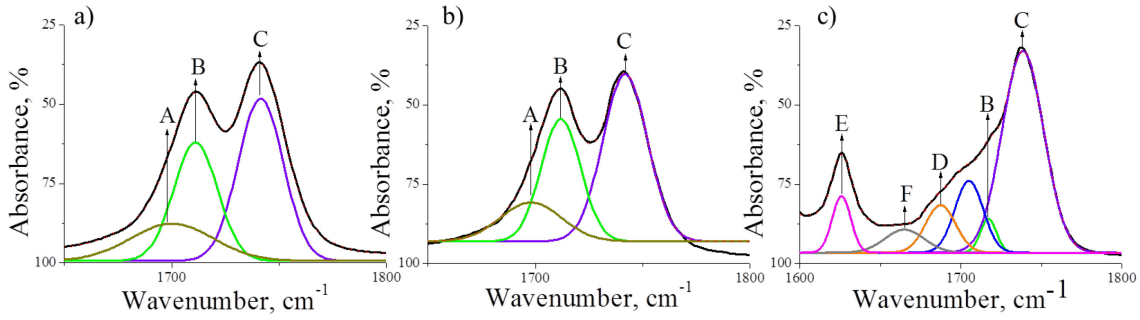

Figure 15. Deconvoluted carbonyl region of FTIR spectra for samples containing equal molar ratio DMPA:PCD in a form of PU nanoparticles in acetone: a) 1.05 NCO excess, b) 1.5 NCO excess and c) sample after water addition containing 1.5 NCO excess. The marked peaks are attributed to: A – free urea, B – hydrogen-bonded urethane, C – free urethane, D – biuret and hydrogen-bonded carbonate, E – strongly bonded urea, F – weakly bonded urea.

After water addition, no significant changes in samples containing 1.05 NCO excess were noticed. However, in the series with 1.5 NCO excess, water-crosslinking was observed as a formation of new band D attributed to biuret groups (Fig. 15c)) and bonded urea (band E and F). The highest intensity of the peak corresponding to biuret groups was detected for sample containing the highest amount of DMPA, suggesting the highest crosslinking density among samples with 1.5 NCO excess. This behavior may be explained by the highest HDI amount used for preparation of this sample, leading to the highest number of possible junction points. The opposite result was noticed for PUD with the highest concentration of PCD, forming the weakest biuret peak and the strongest urea band intensity. This suggests that in this sample the chain extension by urea formation dominates over the crosslinking by biuret formation. Thus, the main crosslinking of this sample takes a place in acetone, in the first step of the synthesis.

The investigation of crosslinks formation was carried out also by DMTA analyses for samples containing 1.5 NCO excess. Before water addition step, the highest crosslinking density revealed sample with the highest PCD amount, as a result of the highest number of long polymer chains and hydrogen bonding possibilities. Thus, the distance between the PU nanoparticles was short enough to form the polymer network easily. During the water addition, both crosslinking as well as the phase inversion take a place, creating hydrophobic core consisting of PCD surrounded by hydrophilic shell created by DMPA. The same sample with the highest PCD concentration did not show

difference in crosslinking density between the first and the second reaction step, confirming that the main crosslinking reactions occurs in the first monitored stage. This behavior was caused by the highest amount of hydrophobic segments, reducing water penetration into PU nanoparticles. While considering the sample containing the highest concentration of DMPA, the significant increasing of crosslinking density after water addition was noticed. This can be explained by high amount of short and more hydrophilic NCO-terminated chains in acetone, which easily react with water to form biuret crosslinks.

The PU nanoparticles were further analyzed by light scattering methods (SLS and DLS). The particle shapes in the acetone dispersions were estimated by calculation of the ratio R_g/R_H. It was concluded that PUs containing 1.05 NCO excess feature rod-like morphology in the first step of the reaction. In turn, the samples with 1.5 NCO excess and the highest and medium PCD amount are characterized by the R_g/R_H ratio typical for compact spheres, whereas the nanoparticles containing the highest DMPA concentration create microgel. Moreover, the sample with the highest DMPA amount is the most swellable in acetone, confirming the lowest crosslinking density in the series with 1.5 NCO excess. The changes in the PU morphology toward compact spheres with increasing of PCD amount are caused by differences in the polymer chain lengths.

The self-assembly of PUs in the second step of synthesis, after water addition and acetone removal, was monitored by DLS measurements of the aqueous dispersions. Since PUs contain hydrophilic and hydrophobic parts, in the second step the nanoparticles create core-shell structures as a result of the phase inversion. While considering samples with 1.05 NCO excess, in the case of using the highest amount of PCD, the biggest particles are detected due to the highest amount of long polymer chains. Simultaneously, these nanoparticles are the least stable in water because of the lowest number of ionic groups. In the series with 1.5 NCO excess, additional water-crosslinking takes a place at the same time. The comparison of linear and crosslinked particles revealed higher values of R_g and lower ζ for 1.5 NCO excess, concluding extension of the nanoparticles after water-crosslinking.

The above results allowed purposing of a structural model of the PUs self-assembly (Scheme 7). It was concluded, that all PU nanoparticles with 1.05 NCO excess contain randomly located HS and SS (Scheme 7a)) due to possibility of dissolution of

both hydrophilic and hydrophobic PU parts in the organic solvent. After water addition, the nanoparticles self-assemble into core-shell structure (Scheme 7b)). The chain lengths of used components, taking into account the molar ratios between them, allowed estimating of the final PU chain lengths. On this basis, the confirmation of the longest PU chains in the series with 1.05 NCO excess was estimated for sample containing the highest PCD amount. When 1.5 NCO excess was used, the nanoparticles were initially crosslinked in the first step of reaction (Scheme 7c)). The highest crosslinking density in these cases was observed while using the highest PCD concentration, due to the lowest distance between long polymer chains. The water addition caused the phase inversion and crosslinking. Since water reacts with NCO groups present at the ends of the chains to give biuret junction points, the mesh sizes can be estimated from the lengths of proper linear PU chains. Thus, the largest mesh sizes and thereby the lowest crosslinking density feature the sample containing the highest PCD amount (Scheme 7d)).

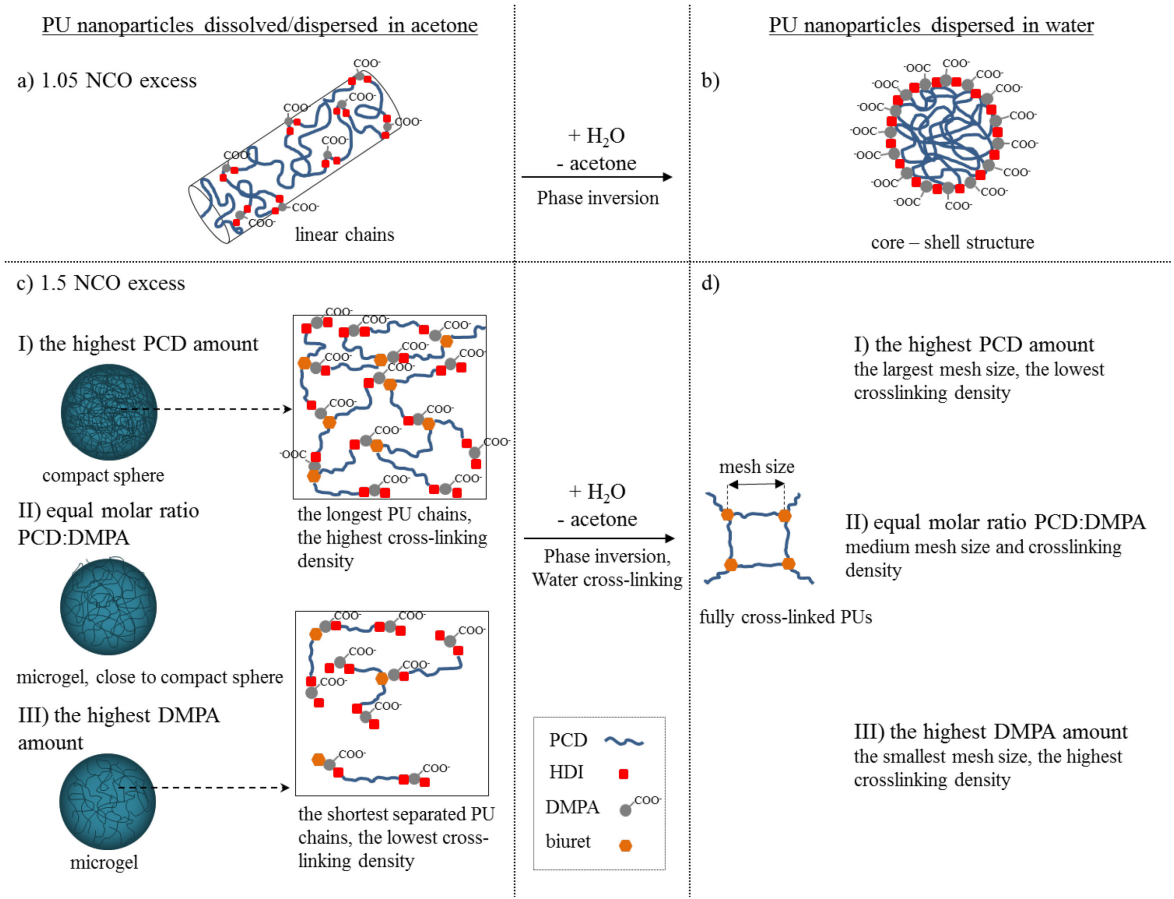

Scheme 7. The self-assembly model of: a) PU with 1.05 NCO excess in acetone and b) in water; c) PU containing 1.5 NCO excess in acetone and d) in water.

The self-assembly of PU nanoparticles was also monitored by AFM analysis of the diluted dispersions deposited on mica (Fig. 16). The elongated disc-shaped particles were observed for samples containing 1.05 NCO excess prepared from acetone solutions (Fig. 16a)). The using of 1.5 NCO excess led to more compact nanoparticles in the first step of reaction (Fig. 16d)), due to their partial crosslinking. All PUDs after water evaporation from the aqueous dispersions (Fig. 16b) and e)) were spherical-shaped, caused by the formation of hydrophilic shell composed of HSs, surrounding hydrophobic SSs. Moreover, estimation of the diameter/height ratio from the AFM images revealed that before water addition the PU nanoparticles containing 1.5 NCO excess were harder than in the series with 1.05 NCO excess due to their higher crosslinking density. The diameter/height ratio decreased after water addition. However, this effect was more significant in the series with 1.5 than 1.05 NCO excess, suggesting that hardness of the nanoparticles is affected more by crosslinking density than core-shell structure formation.

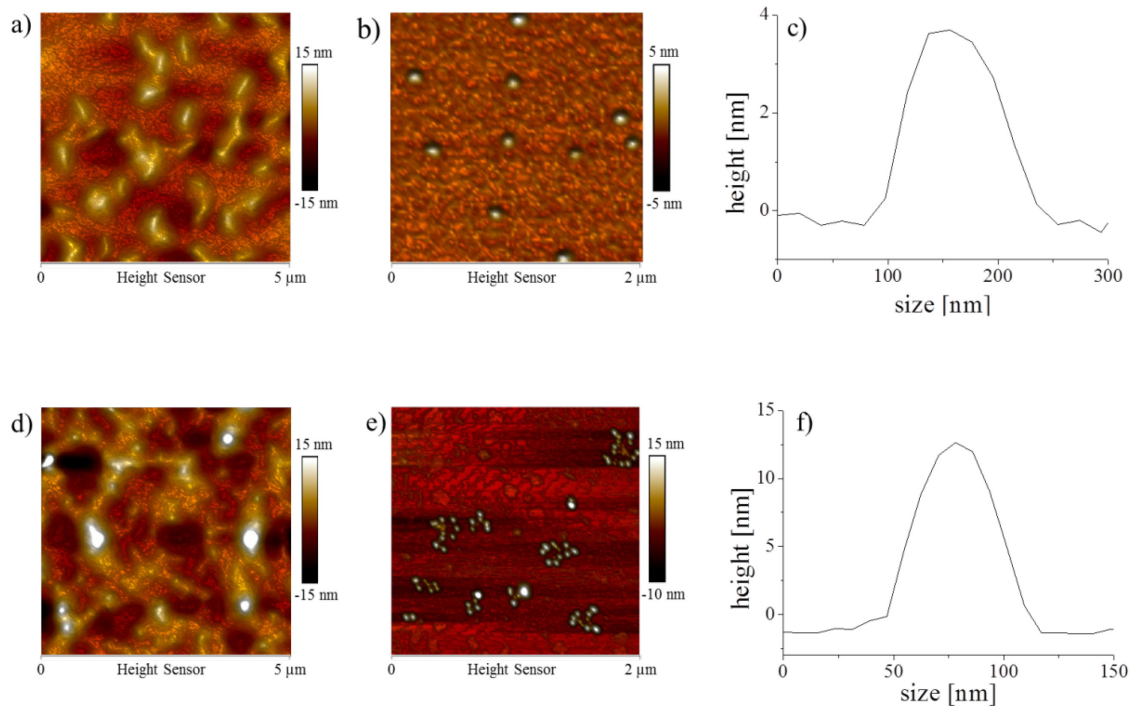

Figure 16. Height AFM images of PU nanoparticles deposited on mica prepared from acetone dispersions containing: a) 1.05 NCO excess, d) 1.5 NCO excess, or from aqueous dispersions: b) 1.05 NCO excess and c) its surface profile, e) 1.5 NCO excess and f) its surface profile.

To summarize, in the fourth paper the PUDs were prepared via modified acetone process. In this technique the chain extension step was eliminated. Moreover, the particles were water-crosslinked. This modification led to more ecofriendly, cheaper and easier for production PUDs. In this study the self-assembly of PU nanoparticles was monitored while using 1.05 NCO excess leading to linear non-water-crosslinked PUs or 1.5 NCO excess forming chemical networks. The investigation was carried out in two steps of the synthesis. It was found that particles containing 1.05 NCO excess are well diluted and rod-like shaped in acetone. After water addition and the phase inversion they create spherical structures. In the cases of using 1.5 NCO excess, the particles are partially crosslinked in acetone forming microgel or compact spheres. However, the final crosslinking and simultaneous phase inversion take a place during water addition, leading to spherical and more compact particles.

4.3. Biostable and biodegradable polyurethane elastomers

4.3.1. Hydrolytically stable aliphatic polyurethanes

The paper V is focused on hydrolytic stability of PU elastomers composed of two types of PCD: T4672 and T5652. The differences between the PCDs were higher regularity and rigidity of T4672 compared to T5652. Other components used for the synthesis were HDI and BD, leading to solely aliphatic linear PUs. Similarly to preparation of PUDs described in the papers I-IV, the isocyanate index was set as 1.05. Moreover, the molar ratios of the components containing hydroxy groups (OH_{PCD} : OH_{BD}) were different, 1 or 2, for control of HSs and SSs amount. After the synthesis, the obtained films were immersed in phosphate-buffered saline (PBS) and investigated under conditions mimicking the physiological conditions (at temperature 37 °C and pH 7.4) for their appearance and resistance after 1, 3, 6 and 12 months.

SEM technique was used for the PU surface study from micrometer to millimeter scales, whereas AFM investigated the morphology in nanometer to micrometer scales. Due to the larger areas possible for measuring by SEM, this method was chosen firstly for characterization of the PU microstructures (Fig. 17). The comparison of PUs based on different PCDs before immersion in PBS showed more regular surface while using more regular PCD (T4672), independently on the ratio OH_{PCD} : OH_{BD} (Fig. 17a) – d)). Moreover, in the all cases films with higher amount of BD led to needle-like structures

(Fig. 17a), c)), whereas increasing of PCD concentration formed spherical formations (Fig. 17b), d)). The inhomogeneity was more visible while using the less regular PCD type (T5652). No significant destructions of the films were found after 12 month-stability test (Fig. 17e) – h)). However, some changes in the morphology were observed. At first, the re-arrangement of the needle-like structures into larger groups (Fig. 17e)) or cubic formations (Fig. 17g)) was noticed. Moreover, in the cases of softer samples containing higher amount of PCD, irregular surface was visible while using PCD T4672 (Fig. 17f)), whereas sample with PCD T5652 showed spherical structures, but more scaly than before the immersion (Fig. 17h)).

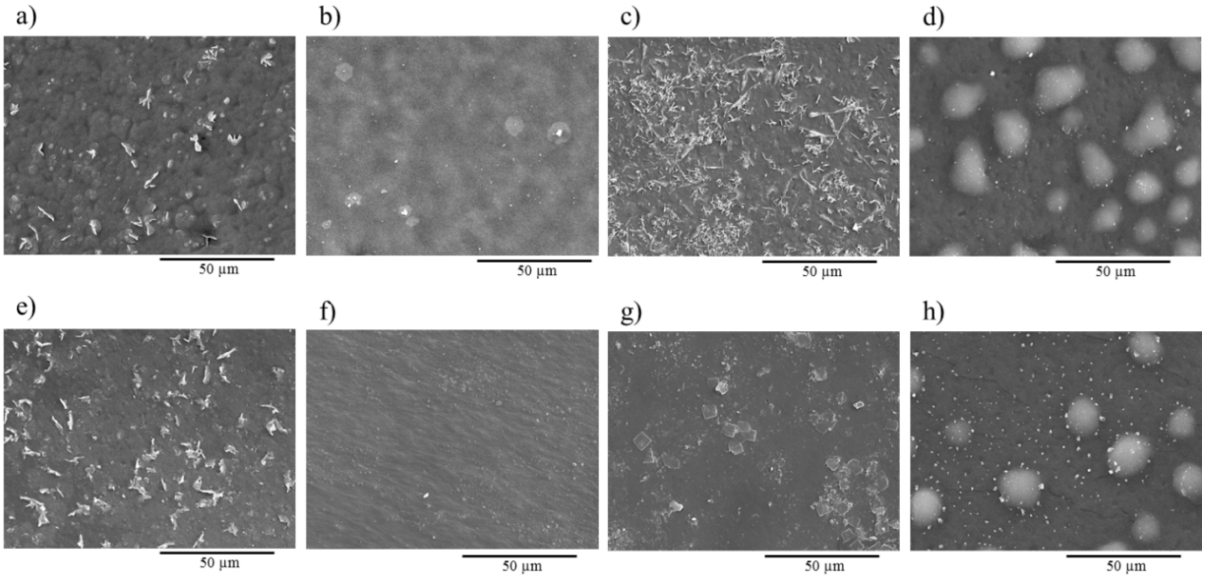

Figure 17. SEM surface analysis of PUs before immersing in PBS: a) based on PCD T4672 and equal molar ratio PCD : BD, b) with two times higher PCD than BD molar ratio; c) based on T5652 and equal molar ratio PCD : BD, d) with two times higher PCD than BD molar ratio; e) – h) corresponding samples after 12 months of the testing.

The sample containing PCD T4672 and equal molar ratio of PCD and BD (Fig. 17a), e)) was chosen for detailed SEM analysis, before the immersion (Fig. 17a)) and after 1, 6 (Fig. 18) and 12 months of testing (Fig. 17e)). The changes in the microstructures can be explained by the re-organization and re-packing of PU chains during immersion of the sample in PBS. Similar cross-section analysis in the all cases (Fig. 18d) – f)) and no visible destructions of the film surfaces were observed, indicating very good hydrolytic stability of the PU elastomers.

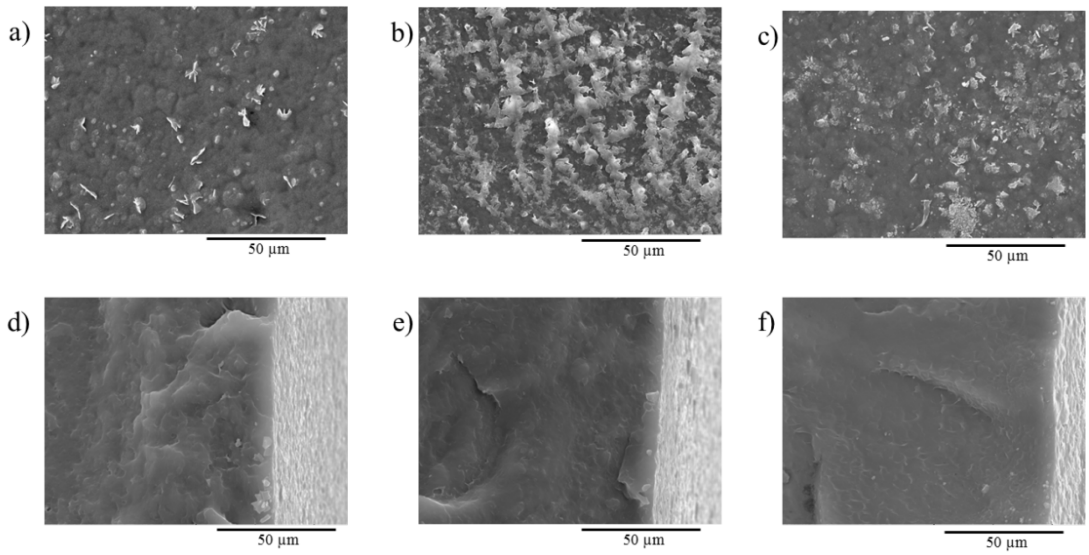

Figure 18. SEM micrographs of the sample based on PCD T4672 and equal molar ratio of PCD : BD investigated for surface analysis: a) before immersion in PBS, b) after 1 month of testing, c) after 6 months; d) – f) the corresponding cross-section images.

The surface and cross-section analyses in higher magnifications were carried out by AFM technique. The same sample extensively characterized by SEM (Fig. 18) was also investigated by AFM after the same time of immersion in PBS (Fig. 19). Due to microphase separation between HSs and SSs, the AFM phase images were proper for monitoring of changes in the PU microstructures. The AFM surface images (Fig. 19a) – c)) were similar to the SEM results (Fig. 18a) – c)), confirming each other. However, the cross-section micrographs (Fig. 19d) – f)) showed spherulites, resulted from self-organization of HSs into supramolecular formations. Detection of the spherulite structures only by AFM is caused by differences between SEM and AFM methods. SEM shows the sample topography only, whereas phase image contrast in AFM is created as a result of differences between hard and soft segments of PUs.

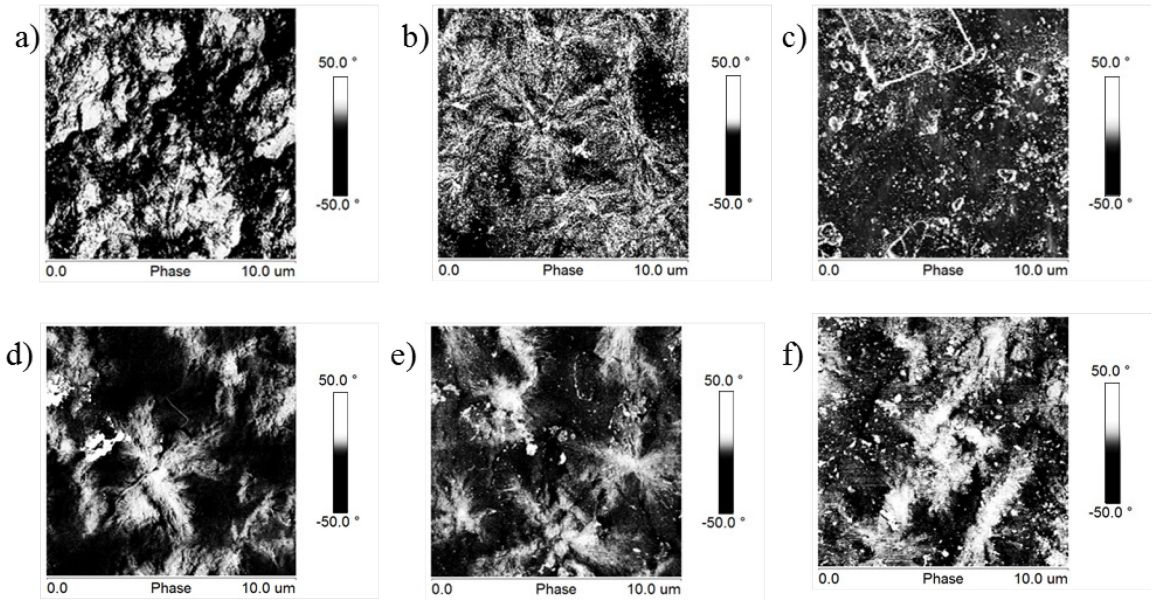

Figure 19. AFM phase images of the sample based on PCD T4672 and equal molar ratio of PCD : BD measured for surface analysis: a) before testing, b) after 1 month of immersion in PBS, c) after 6 months; d) the cross-section analysis before the immersion, e) after 1 month, f) after 6 months of the testing.

The hydrolytic stability of PU elastomers was further investigated by other methods (DSC, tensile testing and water uptake). The same conclusion was obtained after the analyses: PU elastomers based on PCD, BD and HDI are hydrolytically stable and strong materials, characterized by re-organization of their segments during immersion in PBS.

4.3.2. Hydrolytically degradable polyurethane elastomers

The last paper (VI) describes PU elastomers prepared from the same components as in the paper V (PCD, BD and HDI), but additionally a degradable unit (DLL) was incorporated in their structures. It means that the HS composition was unchanged (BD and HDI), whereas SS was based beside on PCD also on DLL. The investigation of the films degradation was carried out at the same conditions as previously. The analyzed samples contained either PCD T4672 or T5652 and equal molar ratio of components containing hydroxy groups (PCD, BD and DLL).

The monitoring of microstructure changes during the degradation tests were carried out for the film surfaces and cross-section analyses by SEM and AFM. The both

microscopic techniques showed relatively smooth surfaces of the untreated PUs (Fig. 20a) and e)). In the almost all cases the immersion in PBS resulted in formations adhered to the film surfaces (Fig. 20c), d), f) – h)). However, no significant destructions of the samples were noticed. This observation confirms the results obtained from other methods of characterization, that the hydrolysis causing the gradual leaching of PU chains from the sample surfaces does not influence significantly their microstructures.

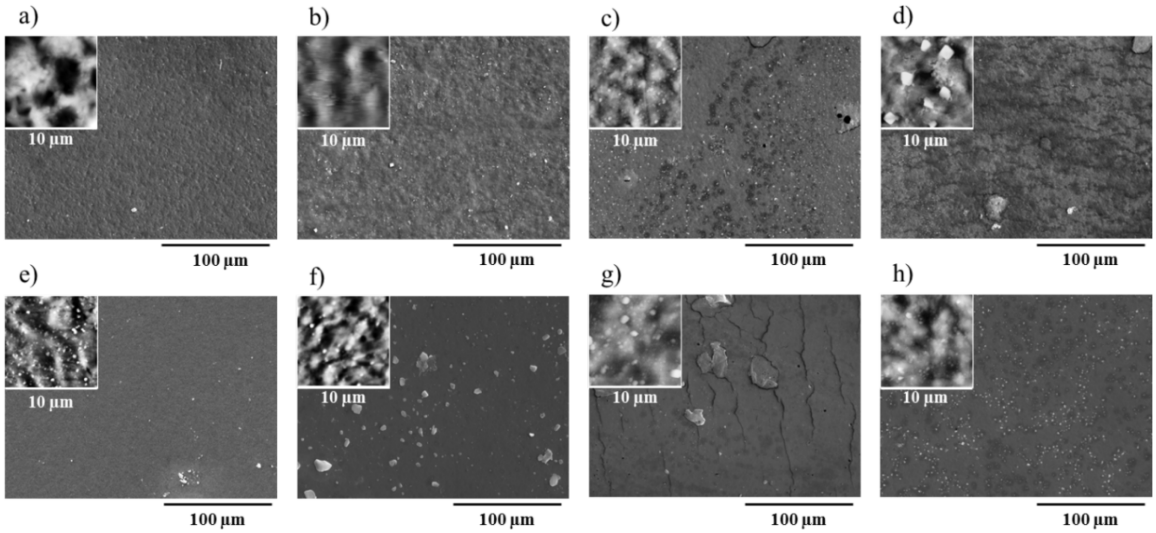

Figure 20. SEM micrographs and AFM height images in upper left corner of PU films containing the degradable unit: a) based on PCD T4672 before immersing in PBS, b) after 3 months, c) after 9 months, d) after 12 months of the testing, e) – f) corresponding samples based on PCD T5652.

The cross-sections of the freeze-fractured films obtained by SEM and AFM were also compared (Fig. 21). No significant cracking during the testing were observed. However, the heterogeneities visible in the phase AFM images were resulted by self-organization of HSs into spherulite structures, characteristic also for PUs without DLL, presented in the paper V. The similarities in morphologies of PUs with or without DLL in their backbone, and simultaneous significant deterioration of mechanical properties for films containing the degradation unit, allow explaining the hydrolytic process. The results imply that the hydrolytic degradation does not affect the highly organized HS domains, but takes a place mainly in the SS region, composed of DLL and PCD, resulted in no significant changes in AFM and SEM images after immersing in PBS.

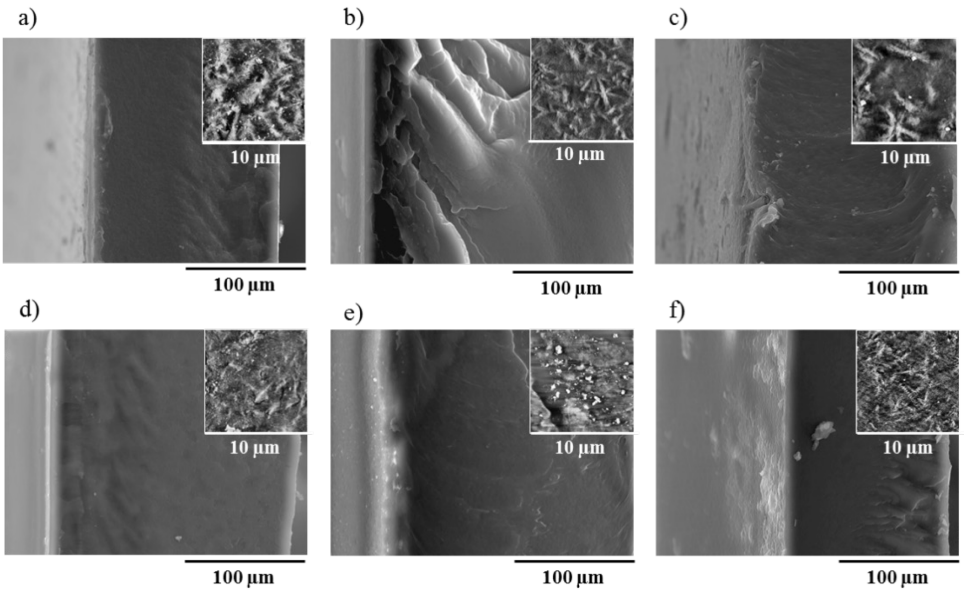

Figure 21. The cross-section analysis of the PU elastomers containing DLL, detected by SEM (left part) and AFM phase contrast (upper right corner): a) based on PCD T4672 before the degradation tests, b) after 6 months, c) after 12 months of the immersing in PBS, d) – f) corresponding samples based on PCD T5652.

To summary, the papers V and VI describe PU elastomers tested for hydrolytic stability under conditions mimicking human body. It was found that polymers made from PCD, BD and HDI are hydrolytically stable up to 12 months of testing. The results were visible for their morphology as well as for other methods of characterization. Moreover, self-organization of HSs during the immersion in PBS was detected by AFM. Further, the degradable unit DLL was incorporated into the PU backbone, enriching the SS composition. It was concluded that DLL accelerates the hydrolytic degradation process, resulted in deterioration of the films resistance during the testing. However, no significant changes in the films microstructures were noticed, indicating that the main degradation does not proceed in highly organized HSs, but in SS domains, hardly to detect by the microscopic techniques.

5. Conclusions.

A new ecofriendly method of PUD-based films preparation from PCD, BD, DMPA and HDI, leading to thermoplastic materials soluble in organic solvents and possible to re-processing, was introduced. The water dispersions were characterized for their stability in aqueous medium and particle size, whereas obtained films were analyzed for their morphology and mechanical, thermal and water resistances.

It was found that the particle size of obtained PUDs varying from 46 nm to 105 nm and ζ-potential being in a range between -65 mV and -29 mV strongly depended on the ionic species provided by DMPA. Increasing of DMPA amount contributed to smaller PU nanoparticles and their better stability in water, whereas higher concentration of BD caused formation of bigger and less stable particles. The antagonistic influence of DMPA and BD was observed for the PUD-based films properties as well. The highest improvement of water resistance was observed for sample contained the highest BD amount as 7 wt% of water uptake, indicating that formation of HSs inhibits water penetration into the materials. In contrast, the PU film with the highest DMPA concentration was the most water sensitive, characterized by 115 wt% of water swelling, showing the negative influence of the ionic groups on the films resistance. Moreover, BD contributed to improvement of the films mechanical properties, from E = 5.9 MPa and σ_b = 1.0 MPa for the lowest BD amount to E = 26.7 MPa and σ_b = 3.7 MPa for the highest BD concentration. However, deterioration of the mechanical resistance was observed with increasing of DMPA amount, as E = 13.9 MPa and σ_b = 1.8 MPa for the highest number of the ionic pairs and E = 3.5 MPa and σ_b = 0.7 MPa for the lowest DMPA concentration. The optimum balance between hydrophobic and hydrophilic segments of the PUDs allows designing them as starting materials for preparation of thermoplastic polymers possible to use in many areas, for example as biodegradable PUs.

The functional properties of the thermoplastic PUD-based films were improved by addition of colloidal silica to PUDs, followed by drying. The main advantages of this method were simplicity, low costs of the nanofillers and the same aqueous medium used both in the PUDs and the colloidal silica sols. It was observed that addition of the nanofiller causes better mechanical, thermal and water resistances compared to the neat matrix. Moreover, silica Ludox AS containing smaller particles turned out to be more compatible with the polymer than silica Ludox TMA, due to formation of higher physical

crosslinking density with PU. The improvement was visible for example as increasing of E from 8 MPa, for the neat matrix to 13 MPa or 10 MPa after addition of 5 wt% of Ludox AS or Ludox TMA, respectively. Addition of the nanofiller significantly increased also T_m of the materials, from 88 °C characteristic for the pure PU to 192 °C or 174 °C for materials containing 32 wt% of Ludox AS or Ludox TMA, respectively. However, all the organic-inorganic PUD-colloidal silica nanocomposites preserved thermoplastic character of the PUs and thus possibility of their recycling.

The synthesis of PUDs was modified by elimination of the chain extension step and water-crosslinking of the PU nanoparticles. The mechanism of linear (containing 1.05 NCO excess) and crosslinked PU nanoparticles (with 1.5 NCO excess) self-assemblies were determined after two steps of the reaction, in acetone and in water. The linear PU nanoparticles found to be rod-like shaped and spherical after water addition, whereas using of 1.5 NCO excess led to formation of partially crosslinked particles in water.

The biostability and biodegradability of PU elastomers with or without the degradable unit were tested under conditions mimicking the physiological environment for the films morphology, measured by SEM and AFM. It was found that PUs are biodegradable only if a biodegradable unit is incorporated into the PU backbone. However, no morphological changes during the testing indicated that the degradation takes a place in SS phase, hard to detect by the microscopic methods. The biodegradable PU elastomers can be used as promising organic matrices for number of nanofillers, to obtain new materials for wide area of applications.

References:

1. O. Bayer, *Angew. Chem.,* **1947**, A59-257.

2. D.K. Chattopadhyay, K.V.S.N. Raju, *Prog. Polym. Sci.,* **2007**, 32, 252-418.

3. N.M.K. Lamba, K.A. Woodhouse, S.L. Cooper, *Polyurethanes in Biomedical Applications,* CRC Press, **1998**.

4. M. Szycher, *Szycher's Handbook of Polyurethanes, Second Edition,* CRC Press, **2013**.

5. S.L. Cooper, J. Guan, *Advances in Polyurethane Biomaterials*, WP Woodhead Publishing, **2016**.

6. C. Prisacariu, *Polyurethane Elastomers: From Morphology to Mechanical Aspects,* Springer, **2011**.

7. G. Behrendt, W. Naber, *J. Chem. Technol. Metall.*, **2009**, 44, 3-23.

8. P. Król, *Prog. Mat. Sci.,* **2007**, 52, 915-1015.

9. U. Meier-Westhues, *Polyurethanes Coatings, Adhesives and Sealants,* Vincentz Network, **2007**.

10. A. Rahimi, A. Mashak, *Plast., Rubber Compos.,* **2013**, 42, 223-230.

11. C. Prisacauri, E. Scortanu, B. Agapie, *Proceedings of the World Congress of Engineering,* **2011**, 3, 2178-2183.

12. C.B. Wang, S.L. Cooper, *Macromolecules*, **1983**, 16, 775-786.

13. J.T. Koberstein, A.F. Galambos, L.M. Leung, *Macromolecules*, **1992**, 25, 6195-6204.

14. J. Yi, M.C. Boyce, G.F. Lee, E. Balizer, *Polymer*, **2006**, 47, 319-329.

15. J.Y. Cherng, T.Y. Hou, M.F. Shih, H. Talsma, W.E. Hennik, *Int. J. Pharm.*, **2013**, 450, 145-162.

16. I.A. Mohammed, G. Sankar, *High Perf. Polym.*, **2011**, 23, 535-541.

17. V. Sekkar, S. Gopalakrishnan, K. Ambika Devi, *Eur. Polym. J.*, **2003**, 39, 1281-1290.

18. A. Lapprand, F. Boisson, F. Delome, F. Méchin, J.P. Pascalut, *Polym. Degrad. Stab.*, **2005**, 90, 363-373.

19. M. Špírková, M. Kubín, K. Dušek, *J. Macromol. Sci. – Chem.*, **1987**, A24, 1151-1166.

20. M. Špírková, M. Kubín, K. Dušek, *J. Macromol. Sci. – Chem.*, **1990**, A27, 509-522.

21. K.S. Chian, L.H. Gan, *J. Appl. Polym. Sci.*, **1998**, 68, 509-515.

22. K. Dušek, M. Špírková, I. Havlíček, *Macromolecules*, **1990**, 23, 1774-1781.

23. P. Ducheyene, *Comprehensive Biomaterials. Metallic, Ceramic and Polymeric Biomaterials, Volume 1,* Elsevier, **2011**.

24. E.J. Goethals, *Telechelic Polymers: Synthesis and Applications*, CRC Press, **1990**.

25. M.F. Sonnenschein, *Polyurethanes: Science, Technology, Markets and Trends,* Wiley, **2015**.

26. J.H. Park, J.Y. Jeon, J.J. Lee, Y. Jang, J.K. Varghese, B.Y. Lee, *Macromolecules*, **2013**, 46, 3301-3308.

27. M.R. Kember, C.K. Williams, *J. Am. Chem. Soc.*, **2012**, 134, 15676-15679.

28. A. Eceiza, M.D. Martin, K. De La Caba, G. Kortaberria, N. Gabilondo, M.A. Corcuera, I. Mondragon, *Polym. Eng. Sci.*, **2008**, 48, 297-306.

29. M. Špírková, J. Pavličević, A. Strachota, R. Poreba, O. Bera, L. Kaprálková, J. Baldrian, M. Šlouf, N. Lazić, J. Budinski-Simendić, *Eur. Polym. J.*, **2011**, 47, 959-972.

30. H.-D. Hwang, C.-H. Park, J.-I. Moon, H.-J. Kim, T. Masubuchi, *Prog. Org. Coat.,* **2011**, 72, 663-675.

31. S.-H. Hsu, Y.-C. Kao, Z.-C. Lin, *Macromol. Biosci.,* **2004**, 4, 464-470.

32. S.-Y. Oh, M.-S. Kang, J.C. Knowles, M.-S. Gong, *J. Biomat. Appl.*, **2015**, 30, 327-337.

33. J.O. Hollinger, *An Introduction to Biomaterials, Second Edition*, CRC Press, **2012**.

34. N. Karak, *Vegetable Oil-Based Polymers: Properties, Processing and Applications*, Woodhead Publishing Limited, **2012**.

35. M. Chiao, J.C. Chiao, *Biomaterials for MEMS*, Pan Stanford Publishing, **2011**.

36. S. Lee, *Thermoplastic Polyurethane Markets in the EU: Production, Technology, Applications and Trends*, Rapra Technology Limited, **1998**.

37. S.R. Hartson, *Structural Adhesives: Chemistry and Techology*, Pleneum Press, **1986**.

38. C. Hepburn, *Polyurethane Elastomers, Second Edition*, Elsevier, **1992**.

39. M. Szycher, C.P. Sharma, *Blood Compatible Materials and Devices: Perspectives Towards the 21st Century*, Technomic Publishing Company, **1991**.

40. F. Gao, *Advances in Polymer Nanocomposites: Types and Applications*, Woodhead Publishing, **2012**.

41. J.G. Drobny, *Handbook of Thermoplastic Elastomers, Second Edition*, Elsevier, **2014**.

42. J.E. Puskas, Y. Chen, *Biomacromolecules*, **2004**, 5, 1141-1154.

43. R.J. Spontak, N.P. Patel, *Curr. Opin. Colloid Interface Sci.*, **2000**, 5, 334-341.

44. H.D. Kim, J.E.H.O. Huh, E.Y. Kim, C.C. Park, *J. Appl. Polym. Sci.*, **1998**, 7, 1349-1355.

45. P.W. Duffon, *Thermoplastic Elastomers*, Rapra Technology Limited, **2001**.

46. A.K. Bhowmick, H. Stephens, *Handbook of Elastomers, Second Edition,* Marcel Dekker, **2001**.

47. D.K. Chattopadhyay, D.C. Webster, *Prog. Org. Sci.*, **2009**, 34, 1068-1133.

48. S. Dedai, I.M. Thakore, B.D. Sarawade, S. Devi, *Eur. Polym. J.*, **2000**, 36, 711-725.

49. P. Alves, J.F.J. Coelho, J. Haack, A. Rota, A. Bruinink, M.H. Gil, *Eur. Polym. J.*, **2009**, 45, 1412-1419.

50. D.A. Dillard, A.V. Pocius, *Adhesion Science and Engineering: The Mechanics of Adhesion*, Elsevier, **2002**.

51. D. Tabuani, F. Bellucci, A. Terenzi, G. Camino, *Polym. Degrad. Stab.*, **2012**, 97, 2594-2601.

52. H. Koerner, W. Liu, M. Alexander, P. Mirau, H. Dowty, R.A. Vaia, *Polymer*, **2005**, 46, 4405-4420.

53. Z.S. Petrović, Y. Xu, Jelena Milić, G. Glenn, A. Klamczynski, *J. Polym. Environ.*, **2010**, 18, 94-97.

54. M.S. Sánchez-Adsuar, *Int. J. Adhesion Adhesives*, **2000**, 20, 291-298.

55. J.P. Theron, J.H. Knoetze, R.D. Sanderson, R. Hunter, K. Mequanint, T. Franz, P. Zilla, D. Bezuidenhout, *Acta Biomaterialia*, **2010**, 6, 2434-2447.

56. B.K. Kim, *Colloid. Polym. Sci.*, **1996**, 274, 599-611.

57. A.D. Wilson, J.W. Nicholson, H.J. Prosser, *Waterborne coatings, Tom 3, Surface coatings*, Elsevier, **1990**.

58. NPCS Board of Consultants & Engineers, *The Complete Book on Water Soluble Polymers*, Asia Pacific Business Press, **2000**.

59. P. Cognard, *Handbook of Adhesives and Sealants: Basic Concepts and High Tech Bonding*, Elsevier, **2005**.

60. D.G. Weldon, *Failure Analysis of Paints and Coatings*, Wiley, **2009**.

61. P. Król, B. Król, R. Stagraczyński, K. Skrzypiec, *J. Appl. Polym. Sci.*, **2013**, 4, 2508-2519.

62. S. Mohanty, N. Krishnamurti, *J. Appl. Polym. Sci.* **1996**, 62, 1993-2003.

63. M.R. Tant, K.A. Mauritz, G.W. Wilkes, *Ionomers: Synthesis, structure, properties and applications*, Blackie Academic & Professional, **1997**.

64. R.A. Pethrick, A. Ballada, G.E. Zaikov, *Handbook of Polymer Research: Monomers, Oligomers, Polymers and Composites*, Nova Science Publishers, **2007**.

65. G. Robilă, I. Diaconu, T. Buruiană, E. Buruiană, P. Coman, *J. Appl. Polym. Sci.*, **2000**, 75, 1385-1392.

66. G. Robilă, M. Ivanoiu, T. Buruiană, E. Buruiană, *J. Appl. Polym. Sci.*, **1997**, 66, 591-595.

67. I. Francolini, L. D'Ilario, E. Guaglianone, G. Donelli, A. Martinelli, A. Piozzi, *Acta Biomaterialia*, **2010**, 6, 3482-3490.

68. J.H. Silver, A.P. Hart, E.C. Williams, S.L. Cooper, S. Charef, D. Labarre, M. Jozefowicz, *Biomaterials*, **1992**, 13, 339-344.

69. X.M. Yang, B.X. Ren, Z.Y. Ren, L. Jiang, W.T. Liu, C.S. Zhu, *J. Mat. Sci. Chem. Eng.*, **2015**, 3, 88-94.

70. C.K. Kim, B.K. Kim, H.M. Jeong, *Colloid Polym. Sci.*, **1991**, 269, 895-900.

71. T.K. Kim, B.K. Kim, *Colloid Polym. Sci.*, **1991**, 269, 889-894.

72. U. Šebenik, M. Krajnic, *J. Polym. Sci. Polym. Chem.*, **2005**, 43, 4050-4069.

73. B.K. Kim, S.Y. Lee, J.S. Lee, S.H. Baek, Y.J. Choi, J.O. Lee, M. Xu, *Polymer*, **1998**, 39, 2803-2808.

74. K.L. Nobe, *Prog. Org. Coat.*, **1997**, 32, 131-136.

75. K. Mequanint, R.D. Sanderson, *Macromol. Symp.*, **2002**, 178, 117-130.

76. A. Eisenberg, B. Hird, R.B. Moore, *Macromolecules*, **1990**, 23, 4098-4107.

77. A. Santamaria-Echart, A. Arbelaiz, A. Saralegi, B. Fernandez-d'Arlas, A. Eceiza, M.A. Corcuera, *Colloids Surf. A: Physicochem. Eng. Aspects*, **2015**, 482, 554-561.

78. U. Path, *Automotive Coatings Formulation*, Vincentz Network, **2008.**

79. L.F.M. da Silva, A. Öchsner, R.D. Adams, *Handbook of Adhesion Technology*, Springer, **2011**.

80. NIIR Board of Engineers & Consultants, *Synthetic Resins Technology Handbook*, Asia Pacific Business Press, **2005**.

81. W.J. Blank, V.J. Tramontano, *Prog. Org. Coat.*, **1996**, 27, 1-15.

82. M. Pilar Montero García, M.C. Gómez-Guillén, M.E. López-Caballero, G.V. Barbarosa-Cánovas, *Edible Films and Coatings: Fundamentals and Applications*, CRC Press, **2017**.

83. M.A. Winnik, *Curr. Opin. Colloid Interface Sci.*, **1997**, 2, 192-199.

84. J. Brander, I. Thorn, *Surface Application of Paper Chemicals*, Blackie Academic and Professional, **1997**.

85. S.R. Senevirathna, S. Amarasinghe, V. Karunarate, M. Koneswaran, L. Karunanayake, *J. Appl. Polym. Sci.*, **2017**, 134, 44475.

86. D.J. Hourston, G. Williams, R. Satguru, J. Padget, D. Pears, *J. Appl. Polym. Sci.*, **1998**, 67, 1437-1448.

87. H.-J. Streitberg, K.-F. Dössel, *Automotive Paints and Coatings, Second, Completely Revised and Extended Edition*, Wiley VCH, **2008**.

88. A. Barni, M. Levi, *J. Appl. Polym. Sci.,* **2003**, 88, 716-723.

89. H. Sardon, L. Irusta, M.J. Fernández-Berridi, J. Luna, M. Lansalot, E. Bourgeat-Lami, *J. Appl. Polym. Sci.*, **2011**, 120, 2054-2062.

90. A.K. Sen, *Coated Textiles: Principles and Applications, Second Edition*, CRC Press, **2008**.

91. Y. Lu, R.C. Larock, *Biomacromolecules*, **2008**, 9, 3332-3340.

92. O. Jaudouin, J.-J. Robin, J.-M. Lopez-Cuesta, D. Perrin, C. Imbert, *Polym. Int.*, **2012**, 61, 495-510.

93. K.K. Rao, M. Ferguson, K. Murphy, J. Zhao, D. Lacks, R. Akolkar, *J. Appl. Electrochem.*, **2016**, 46, 1237-1243.

94. H. Hao, J. Shao, Y. Deng, S. He, F. Luo, Y. Wu, J. Li, H. Tan, J. Li, Q. Fu, *Biomater. Sci.*, **2016**, 4, 1682.

95. J.P. Davim, *The Design and Manufacture of Medical Devices*, Woodhead Publishing, **2012**.

96. R.K. Gupta, E. Kennel, K.-J. Kim, *Polymer Nanocomposite Handbook*, CRC Press, **2010**.

97. J.K. Panday, K.R. Reddy, A.K. Mohanty, M. Misra, *Handbook of Polymernanocomposites. Processing, Performance and Application, Volume A: Layered Silicates*, Springer, **2014**.

98. I.V. Khudyakov, R.D. Zopf, N.J. Turro, *Des. Monomers Polym.*, **2009**, 12, 279-290.

99. Y.I. Tien, K.H. Wei, *Polymer*, **2001**, 42, 3213-3221.

100. S. Zhou, L. Wu, J. Sun, W. Shen, *Prog. Org. Coat.*, **2002**, 45, 33-42.

101. Y. Su, L. Zhao, F. Meng, Q. Wang, Y. Yao, J. Luo, *Colloids Surf. B: Biointerfaces*, **2017**, 152, 238-244.

102. M. Lee, M.H. Heo, H.-H. Lee, Y.-W. Kim, J. Shin, *Carbohyd. Polym.*, **2017**, 159, 125-135.

103. H.C. Prasad, S.A.R. Hashmi, A. Naik, H.N. Bhargaw, *J. Appl. Polym. Sci.*, **2017**, 134, 44389.

104. S. Nayak, T.K. Chaki, D. Khastgir, *Polym. Bull.*, **2017**, 74, 369-392.

105. T. Guruathan, R. Arukula, J.S. Chung, C.R.K. Rao, *Polym. Adv. Technol.*, **2016**, 27, 1535-1540.

106. Z. Petrović, I. Javni, A. Waddon, G. Bánhegyi, *J. Appl. Polym. Sci.*, **2000**, 76, 133-151.

107. S.W. Zhang, R Liu, J.Q. Jiang, C. Yang, M. Chen, X.Y. Liu, *Prog. Org. Coat.*, **2011**, 70, 1-8.

108. M. Ding, J. Li, H. Tan, Q. Fu, *Soft Matter*, **2012**, 8, 5414-5428.

109. A.B. Mathur, T.O. Collier, W.J. Kao, M. Wiggins, M.A. Schubert, A. Hiltner, J.M. Anderson, *J. Biomed. Mater.*, **1997**, 36, 246-257.

110. K. Gorna, S. Gogolewski, *J. Biomed. Mat. Res. A*, **2006**, 79, 128-138.

111. J.P. Santerre, K. Woodhouse, G. Laroche, R.S. Labow, *Biomacromolecules*, **2005**, 26, 7457-7470.

112. S. Podzimek, *Light Scattering, Size Exclusion Chromatography and Asymmetric Flow Field: Powerful Tools for the Characterization of Polymers, Proteins and Nanoparticles*, Wiley, **2011**.

113. F. Jameel, S. Hershenson, *Formulation and Process Development Strategies for Manufacturing Biopharmaceuticals*, Wiley, **2010**.

114. G.W. Padua, Q. Wang, *Nanotechnology Research Methods for Food and Bioproducts*, Wiley-Blackwell, **2012**.

115. W. Jiskoot, D. Crommelin, *Methods for Structural Analysis of Protein Pharmaceuticals*, American Association of Pharmaceutical Scientists, **2005**.

116. J. Koetz, S. Kosmella, *Polyelectrolytes and Nanoparticles*, Springer, **2007**.

117. J.E. Mark, H.R. Allcock, R. West, *Inorganic Polymers, Second Edition*, Oxford University Press, **2005**.

118. Y. Gonanou, M. Fontanille, *Organic and Physical Chemistry of Polymers*, Wiley, **2008**.

119. G. Knapp, *Atomic Force Microscopy, Scanning Nearfield Optical Microscopy and Nanoscratching: Application to Rough and Natural Surfaces*, Springer, **2006**.

120. B. Voigtläender, *Scanning Probe Microscopy: Atomic Force Microscopy and Scanning Tunneling Microscopy*, Springer, **2015**.

121. P.C. Braga, D. Ricci, *Atomic Force Microscopy: Biomedical Methods and Applications*, Human Press, **2004**.

122. R. Reifenberg, *Fundamentals of Atomic Force Microscopy: Part I: Fundations*, World Scientific, **2016**.

123. W.R. Bowen, N. Hilal, *Atomic Force Microscopy in Process Engineering: An Intoduction to AFM for Improved Processes and Products*, Elsevier, **2009**.

124. A.M. Baró, R.G. Reigenberg, *Atomic Force Microscopy in Liquid: Biological Applications*, Wiley, **2012**.

125. D.E. Chandler, R.W. Roberson, *Bioimaging: Current Concepts in Light and Electron Microscopy*, Jones and Bartlett Publishers, **2009**.

126. G. Dehm, J.M. Howe, J. Zweck, *In-situ Electron Microscopy: Applications in Physics, Chemistry and Materials Science*, Wiley, **2012**.

127. J. Goldstein, D.E. Newbury, D.C. Joy, C.E. Lyman, P. Echlin, E. Lifshin, L. Sawyer, J.R. Michael, *Scanning Electron Microscopy and X-ray Microanalysis: Third Edition*, Springer Science + Business Media, **2003**.

128. T. Whelan, *Polymer Technology dictionary, Chapman & Hall*, **1994**.

129. M. Gromada, G. Mishurvis, A. Öchsner, *Correction Formulae for Stress Distribution in Round Tensile Specimens at Neck Presence*, Springer, **2011**.

130. J.R. Davis, *Tensile Testing, Second Edition*, ASM International, **2004**.

131. K.P. Menard, *Dynamic Mechanical Analysis: A Practical Introduction, Second Edition*, CRC Press, **2008**.

132. M.P. Sepe, *Thermal Analysis of Polymers,* Rapra Technology LTD, **1997**.

133. J. Scheirs, *Compositional and Failure Analysis of Polymers: A Practical Approach*, Wiley, **2000**.

134. R. Kotsilkova, *Thermoset Nanocomposites for Engineering Applications*, Smithers Rapra Technology Limited, **2007**.

LIST OF PUBLICATIONS

Impacted publications:

1. M. Serkis, R. Poręba, J. Hodan, J. Kredatusová, M. Špírková, "Preparation and characterization of thermoplastic water-borne polycarbonate-based polyurethane dispersions and cast films", *J. Appl. Polym. Sci.,* **2015**, 132, 42, 42672.

2. M. Špírková, L. Machová, L. Kobera, R. Poręba, M. Serkis, A. Zhigunov, "Multiscale approach to the morphology, structure, and segmental dynamics of complex degradable aliphatic polyurethanes", *J. Appl. Polym. Sci.,* **2015**, 132, 10, 41590.

3. R. Poręba, J. Kredatusová, J. Hodan, M. Serkis, M. Špírková, "Thermal and mechanical properties of multiple-component aliphatic degradable polyurethanes, *J. Appl. Polym. Sci.,* **2015**, 132, 16, 41872.

4. M. Serkis, M. Špírková, R. Poręba, J. Hodan, J. Kredatusová, D. Kubies, „Hydrolytic stability of polycarbonate-based poluurethane elastomers tested in physiologically simulated conditions", *Polym. Degrad. Stabil.*, **2015**, 119, 23-34.

5. M. Serkis, M. Špírková, J. Kredatusová, J. Hodan, R. Bureš, „Organic-inorganic nanocomposite films made from polyurethane dispersions and colloidal silica particles", *Compos. Interfaces*, **2016**, 23, 2, 157-173.

6. M. Špírková, M. Serkis, R. Poręba, L. Machová, J. Hodan, J. Kredatusová, D. Kubies, A. Zhigunov, „Experimental study of the simulated process of degradation of polycarbonate- and D,L-lactide-based polyurethane elastomers under conditions mimicking the physiological environment", *Polym. Degrad. Stabil.*, **2016**, 125, 115-128.

7. M. Serkis, M. Špírková, J. Hodan, J. Kredatusová, „Nanocomposites made from thermoplastic polyurethane and colloidal silica. The influence of nanosilica type on the functional properties", *Prog. Org. Coat.*, **2016**, 110, 342-349.

8. M. Perchacz, H. Beneš, A. Zhigunov, M. Serkis, E. Pavlova, "Differently-catalyzed silica-based precursors as functional additives for the epoxy-based hybrid materials", *Polymer*, **2016**, 99, 434-446.

9. M. Špírková, J. Hodan, L. Kobera, J. Kredatusová, D. Kubies, L. Machová, R. Poręba, M. Serkis, A. Zhigunov, J. Kotek, "The influence of the length on the degradable segment on the functional properties and hydrolytic stability of multi-component polyurethane elastomeric films", *Polym. Degrad. Stabil.*, **2017**, 137, 216-228.

10. M. Serkis-Rodzeń, M. Špírková, P. Matějíček, M. Štěpánek, "Formation of linear and crosslinked polyurethane nanoparticles that self-assemble differently in acetone and in water", *Prog. Org. Coat.*, **2017**, 106, 119-127.

APPENDICES I-IV

Waterborne polyurethanes and films based on polyurethane water dispersions:

(I) M. Serkis, R. Poręba, J. Hodan, J. Kredatusová, M. Špírková, "Preparation and characterization of thermoplastic water-borne polycarbonate-based polyurethane dispersions and cast films", *J. Appl. Polym. Sci.,* **2015**, 132, 42, 42672.

(II) M. Serkis, M. Špírková, J. Kredatusová, J. Hodan, R. Bureš, „Organic-inorganic nanocomposite films made from polyurethane dispersions and colloidal silica particles", *Compos. Interfaces*, **2016**, 23, 2, 157-173.

(III) M. Serkis, M. Špírková, J. Hodan, J. Kredatusová, „Nanocomposites made from thermoplastic polyurethane and colloidal silica. The influence of nanosilica type on the functional properties", *Prog. Org. Coat.*, **2016**, 110, 342-349.

(IV) M. Serkis-Rodzeń, M. Špírková, P. Matějíček, M. Štěpánek, "Formation of linear and crosslinked polyurethane nanoparticles that self-assemble differently in acetone and in water", *Prog. Org. Coat.*, **2017**, 106, 119-127.

APPENDICES V, VI

Biostable and biodegradable polyurethane elastomers:

(V) M. Serkis, M. Špírková, R. Poręba, J. Hodan, J. Kredatusová, D. Kubies, „Hydrolytic stability of polycarbonate-based poluurethane elastomers tested in physiologically simulated conditions", *Polym. Degrad. Stabil.*, **2015**, 119, 23-34.

(VI) M. Špírková, M. Serkis, R. Poręba, L. Machová, J. Hodan, J. Kredatusová, D. Kubies, A. Zhigunov, „Experimental study of the simulated process of degradation of polycarbonate- and D,L-lactide-based polyurethane elastomers under conditions mimicking the physiological environment", *Polym. Degrad. Stabil.*, **2016**, 125, 115-128.